Real-time Hydro-environmental Modelling and Visualization System for Public Engagement (ITS/071/06)

Technical Note on Validation of the 3D flow and mass transport model (EFDC/DESA)

K.W. Choi, J.Q. Mao and J.H.W. Lee
Croucher Laboratory of Environmental Hydraulics
Department of Civil Engineering
The University of Hong Kong
November 2007

1 Introduction

The simulation engine of the present system is based on the three-dimensional (3D) flow model with the Distributed Entrainment Sink Approach (DESA) for near and far field coupling (Choi and Lee 2007). The far field flow and mass transport model is based on the Environmental Fluid Dynamics Code (EFDC) that solves the free surface flow and transport problems (Hamrick 1992). EFDC is a finite difference model that solves the shallow water equations using the Mellor and Yamada (1982) scheme for turbulent closure. The system of governing equations including the continuity, momentum and transport equations provides a closed system for the variables including the flow velocity components U, V, W, water surface elevation above the mean sea level η, fluid density ρ, salinity S, temperature T and pollutant concentration C. The pressure P is assumed to be hydrostatic and consists of barotropic (induced by external free surface gravity) and baroclinic (induced by the horizontal density gradient) components. The model uses a staggered grid for discretization and a σ grid co-ordinate in vertical direction. The modal splitting technique is used to solve the discretized equations and the model simulation is separated into the external and internal modes. Without sacrificing the accuracy, this approach allows the calculation of the free surface elevation by solving the vertically integrated horizontal transport (external mode) separately from the 3D computation of the velocity, salinity, temperature and pollutants (internal mode).

To verify that the simulation engine for the simulation and visualization system can produce satisfactory simulation for Hong Kong Waters, numerical models have been constructed and tested for the salinity intrusion problem in estuary with rectangular section, Tolo Harbour, Port Shelter and Victoria Harbour. The computed results are compared with the available field observation and those obtained by the industrial standard commercial software, Delft3d. The following is the summary of the test results.

For the water quality simulations, besides conservative tracer or pollutant, bacteria concentration in term of *E. coli* is also modelled. The formulation of the mortality of *E. coli* is based on the commonly used Mancini (1987) approach:

$$k = (k_b + k_s S)\,\theta_T^{T-20} + k_I I \left(\frac{1 - e^{-e_t H}}{e_t H}\right)$$

where k = first order mortality rate of coliform (d^{-1}), k_b = basic mortality rate (d^{-1}), k_s = salinity related mortality coefficient ($\mathrm{ppt}^{-1}\mathrm{d}^{-1}$), S = salinity (ppt), θ_T = temperature coefficient of the mortality rate, T = temperature ($^\circ$ C), k_I = radiation related mortality coefficient ($\mathrm{m}^2\mathrm{W}^{-1}\mathrm{d}^{-1}$), I = daily solar UV-radiation at the water surface (Wm^{-2}) (= $f_{UV} I_0$ with f_{UV} = fraction of UV-

radiation in visible light = 0.45 and I_0 = daily solar radiation at the water surface), e_t = extinction of radiation (m^{-1}) and H = water depth (m) respectively.

2 Salinity intrusion in estuary of rectangular section

To test that the 3D hydrodynamic model can properly simulate the salinity transport in an estuary under the action of tide and freshwater runoff, the salinity intrusion in a rectangular estuary can be used as the test case. Ippen and Harleman (1961) have described the results of a series of salinity intrusion experiments conducted in a tidal flume. The channel is 327 ft. (99.67 m) long, 0.75 ft. (0.2886 m) wide and 1.5 ft. (0.4572 m) deep. The mean depth is kept at 0.5 ft. (0.1524 m) for all test runs discussed. Tides are generated by means of a large skimming weir in the tidal basin. Constant salinities are maintained at this end to represent the ocean end of the idealized estuary during each test run. Constant freshwater is discharged into the estuary at the other end of the channel. The flume is operated for sufficient long to achieve mean steady state conditions for salinity intrusion. The experiment results provided in the reference are used to verify that the 3D flow model is capable to reproduce the salinity transport in the estuary resulting from the salinity difference existing between the open sea and the freshwater inflow along the intrusion length.

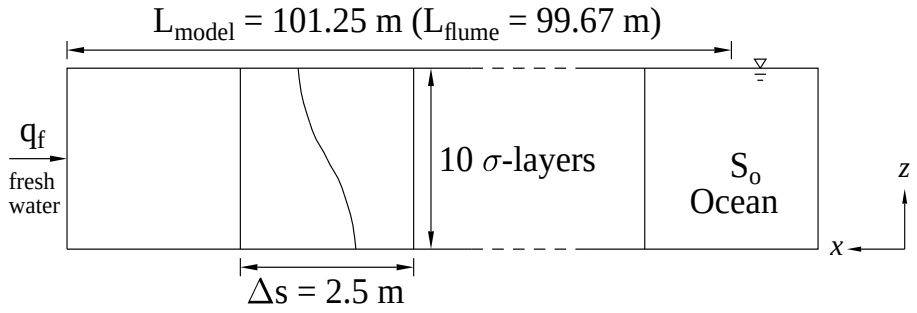

Figure 1: Numerical model for salinity intrusion in a tidal flume

Four cases are selected and presented below. The basic characteristics of the test runs carried out are listed in the following table and the original test no. for the experiment is used as the test case reference. All the length scales have been converted from British unit into Metric unit. It can be noted that for test 2 and 16, the same tidal amplitude is used but different freshwater discharges are applied, while for test 14 and 16, the same freshwater discharge is used, but different tidal amplitudes are applied at the ocean end (Fig 1).

Test no.	Ocean salinity S_o (ppt)	Freshwater discharge per unit width q_f (m^2/s)	Tidal amplitude a (m)
29	0.0	0.0	0.01524
2	25.6	1.858 x 10^{-3}	0.01524
14	29.7	0.929 x 10^{-3}	0.03048
16	29.2	0.929 x 10^{-3}	0.01524
Tidal period T = 600 sec.			

A model of grid size 2.5 m × 0.2886 m and 10 vertical layers is used to model the flume channel. A schematic diagram for the model set-up is given in Fig 1. The modelled flume is slightly longer

than the actual flume. At the upstream end, discharge boundary condition is applied. Freshwater with zero salinity is introduced evenly into the 10 layers. At the downstream or ocean end, tidal boundary condition is prescribed. For a flood tide, the inflow salinity is the specified ocean salinity, while for an ebb tide, the outflow salinity is the salinity at interior cell near to the ocean boundary.

The time step for the simulations is 1 sec. All the model simulations are 'cold' started, i.e. all surface elevations and velocities are taken to be zero initially. It takes about 30 to 40 tidal cycles for the numerical model to reach the quasi-steady state (the difference between the results of consecutive tidal cycle is less than 1 %). Since the actual and modelled flume is not exactly the same length, so relative length along the channel is used in the comparisons between the experimental and computed results. Fig 2 shows the measured and computed water levels for Test 29 along the flume at High Water (HW) and Low Water (LW).

The instantaneous depth-averaged salinity distributions for the test cases 16, 2, and 14 are shown in Fig 3a) and Fig 4. It can be seen that there are satisfactory agreement between the model results and the experimental measurements. The minimum and maximum intrusion extent at LW and HW respectively have been well predicted. Information on the vertical salinity distribution is only available for Test 16. Fig 3b) shows the computed and observed tidally averaged vertical salinity profiles at selected locations. The observations are made at 5 ft., 40 ft., 80 ft., 120 ft. and 160 ft. from the ocean boundary. The distance is used as the reference for the station as indicated in the figure. As, these measurement points do not coincide with the model grid, so the model results have been interpolated for the purpose of comparison. These figures indicate that the model have reproduced the observed vertical salinity distribution reasonably well. The computed results by Delft3d for test case 16 are also shown in Fig 3). It can been seen that both models agree well with the laboratory results, and the differences between the computed results are probably due to the different turbulence closure schemes being employed (Mellor-Yamada vs. k-ϵ).

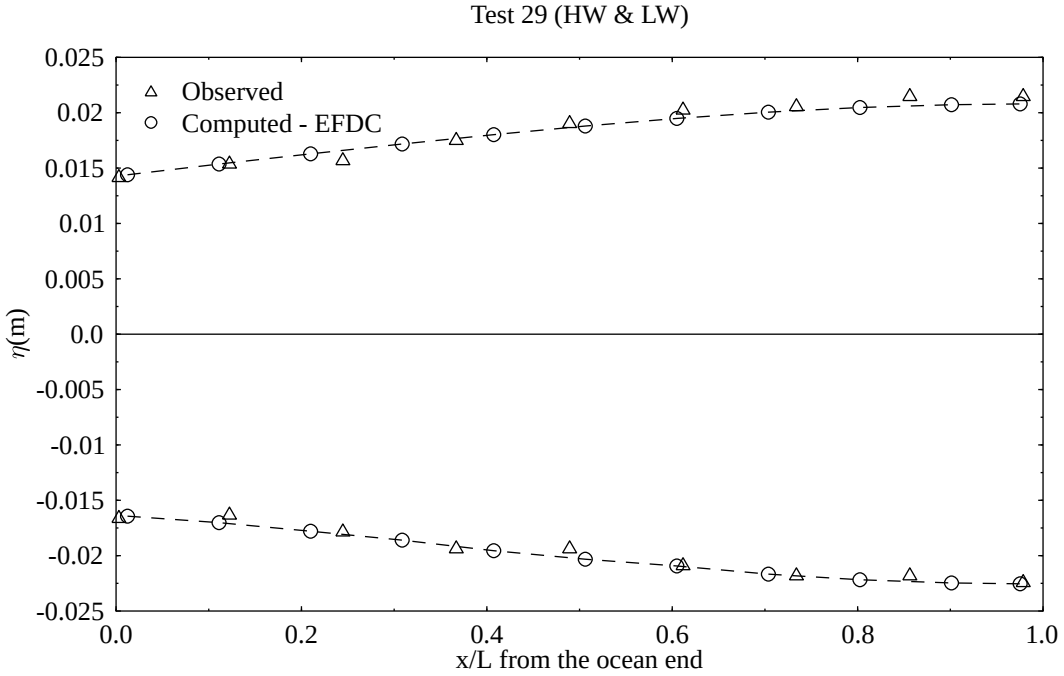

Figure 2: Comparison of experimental and computed tidal levels for Test 29

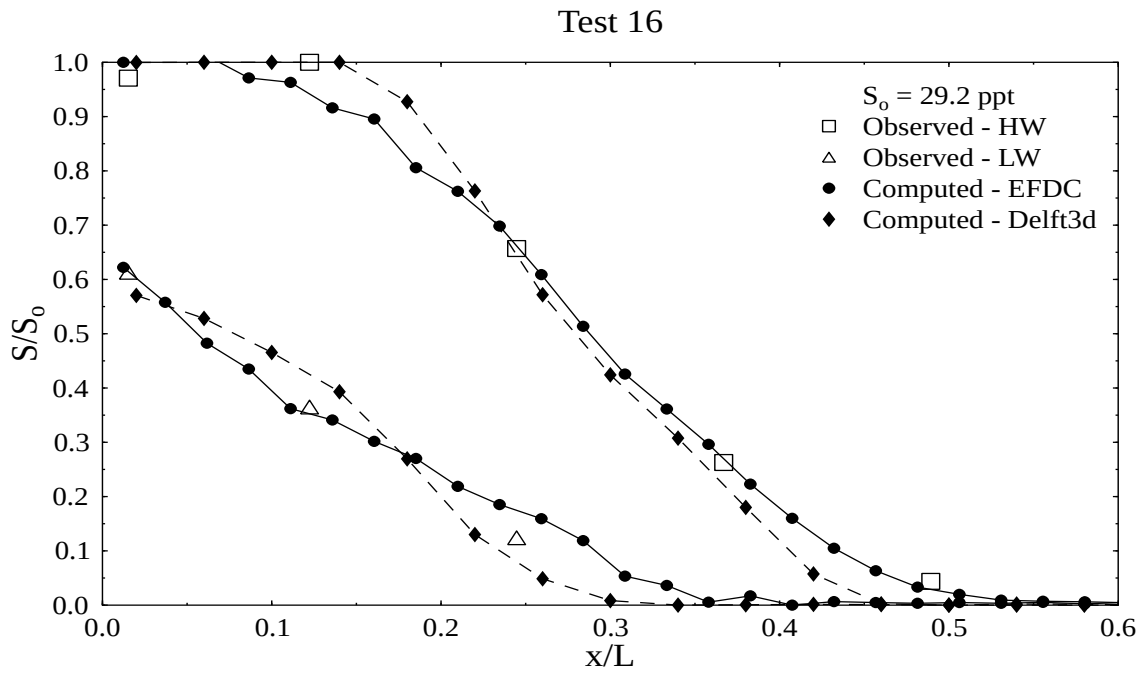

a) Instantaneous depth-averaged salinity distributions

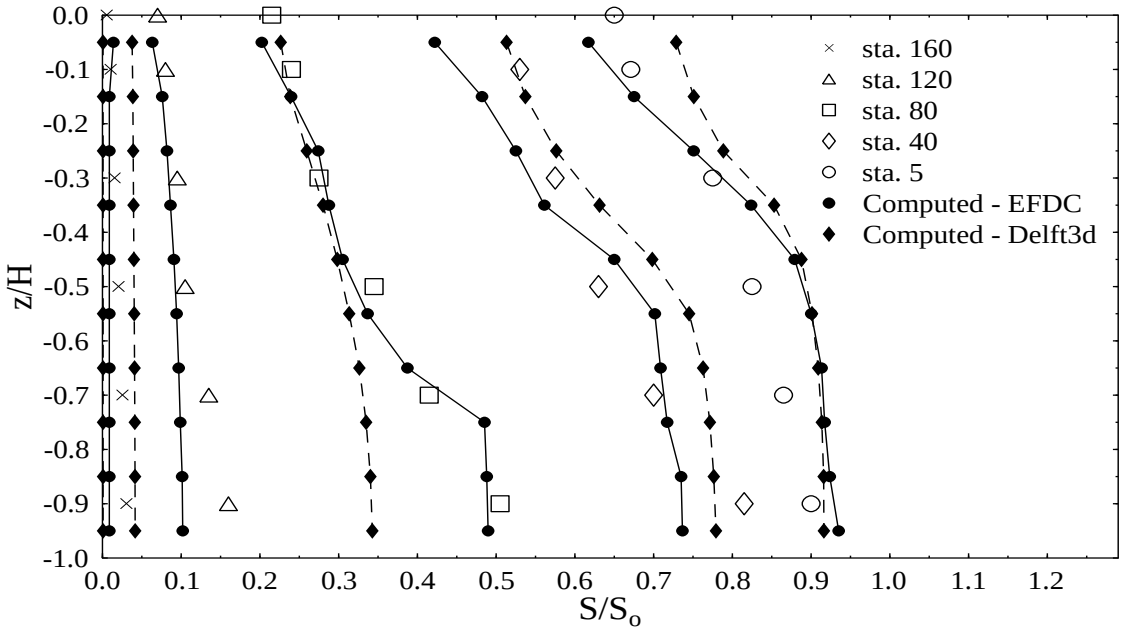

b) Tidally average salinity/ocean salinity vs. relative depth

Figure 3: Comparison of experimental and computed salinity for Test 16

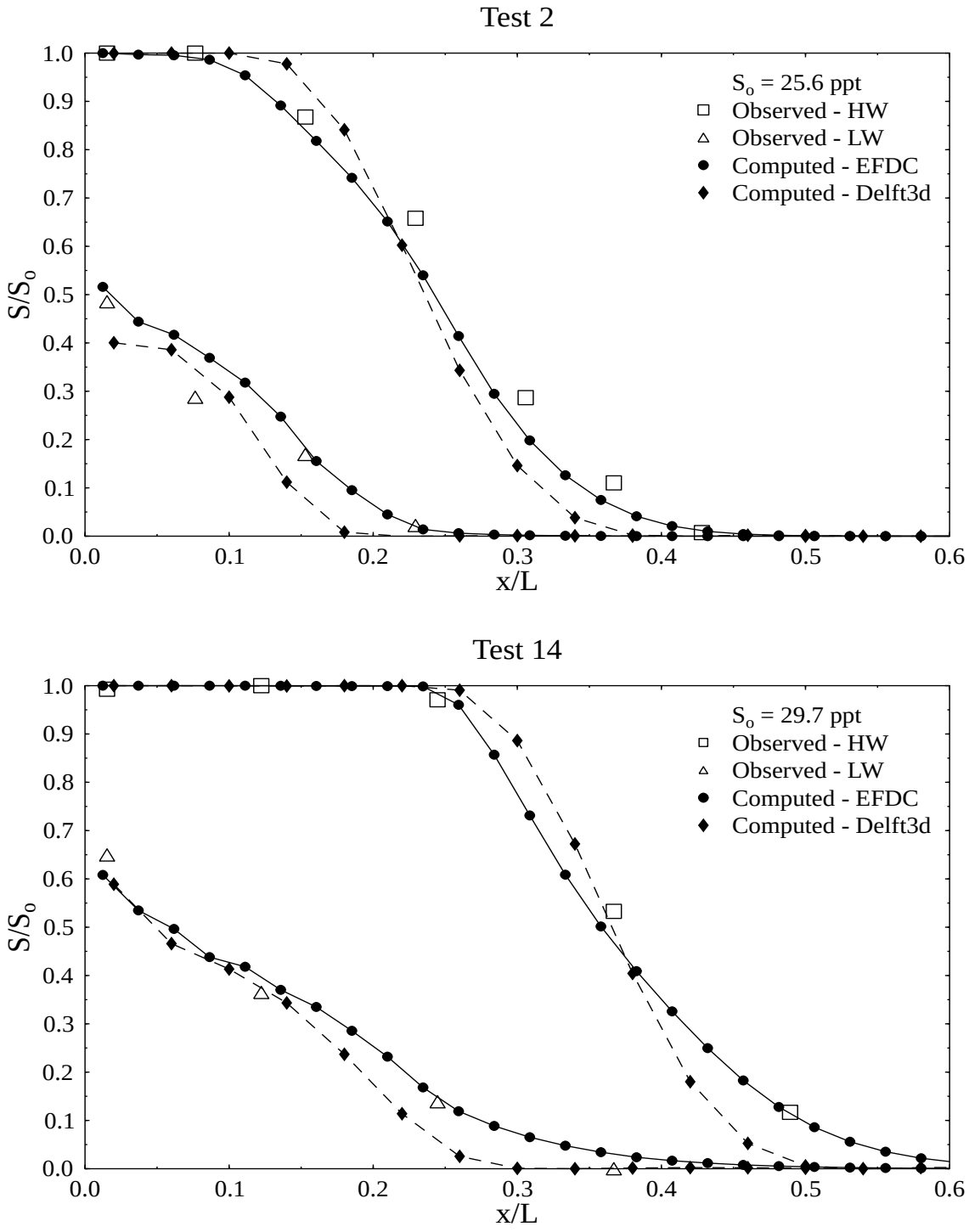

Figure 4: Instantaneous depth-averaged tidally averaged salinity distribution for Test 2 and 14

3 Pollution discharge in estuary of rectangular section

To further check the consistency between the EFDC model and the Delft3d model, flow and mass transport simulations in a straight rectangular estuary have been carried out. The channel is assumed to be 8,000 m long, 1,250 m wide and 15 m deep. It is closed at one end, while the tidal forcing at the open boundary is assumed to be a S2 tide with amplitude of 0.85 m and period of 12 hours. The model uses a 33 $\times$ 5 $\times$ 10 uniform grid and has 160 active horizontal cells (Fig. 5). Each horizontal cell is 250 m $\times$ 250 m.

Two flow scenarios are carried out: unstratified and stratified case. For the unstratified case, a constant salinity of 32 ppt is considered. For stratified case, a linear vertical salinity variation is assumed at the open boundary. The surface and bottom salinity are assumed to be 30 and 34 respectively (Fig. 6). As shown in Fig. 7 & 8, the computed velocities by the two models are almost identical for both cases.

To simulate the mass transport, an effluent discharge of 2.0 m^3/s (or 172,800 m^3/d) is introduced at the location shown in Fig. 5. From Fig. 9 & 10, it can be seen that for the unstratified case the simulated results are very close if the pollution sources are added to all the layers uniformly at the location of the outfall, but there are some discrepancies for the stratified case. When the effluent discharge is represented by a single source at the surface, greater differences between the two models are found (Fig. 11 & 12), but the differences are in general well within 10%. These again indicate that the difference between the results of the two models are related to the different representation for vertical mixing.

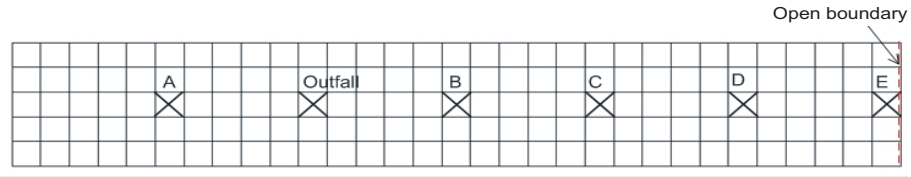

Figure 5: Numerical model for tidal estuary of rectangular section

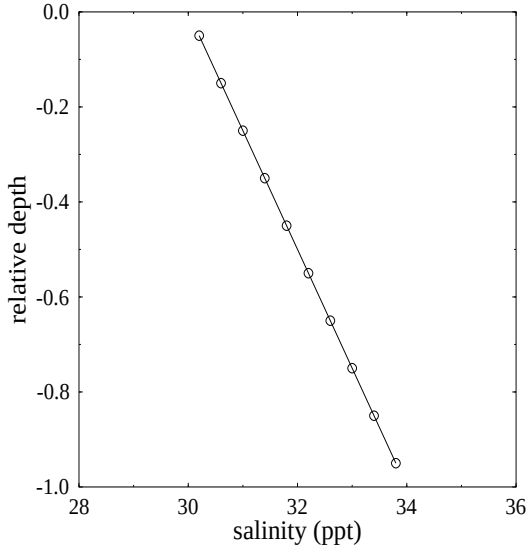

Figure 6: Vertical salinity profile assumed (stratified tidal flow) at open boundary

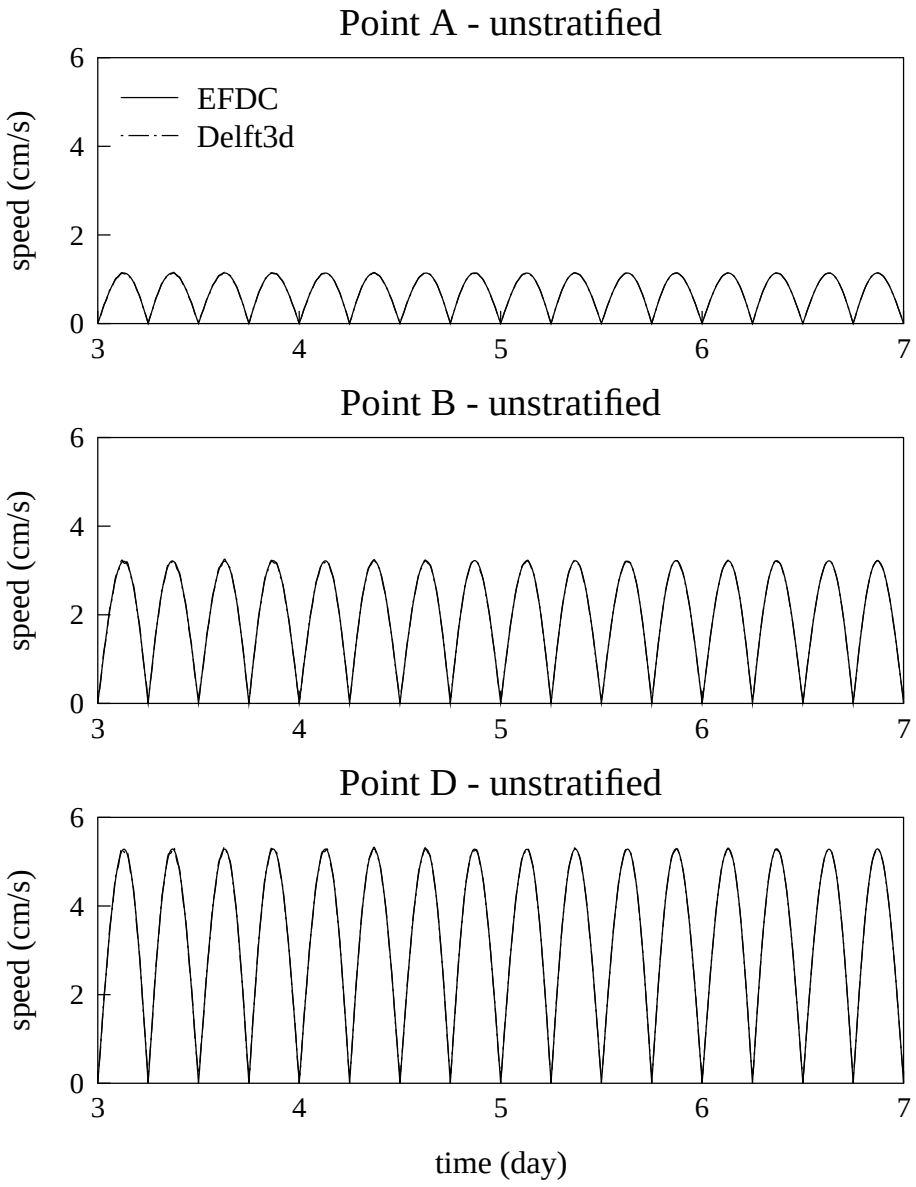

Figure 7: Computed speed for unstratified tidal flow in rectangular channel

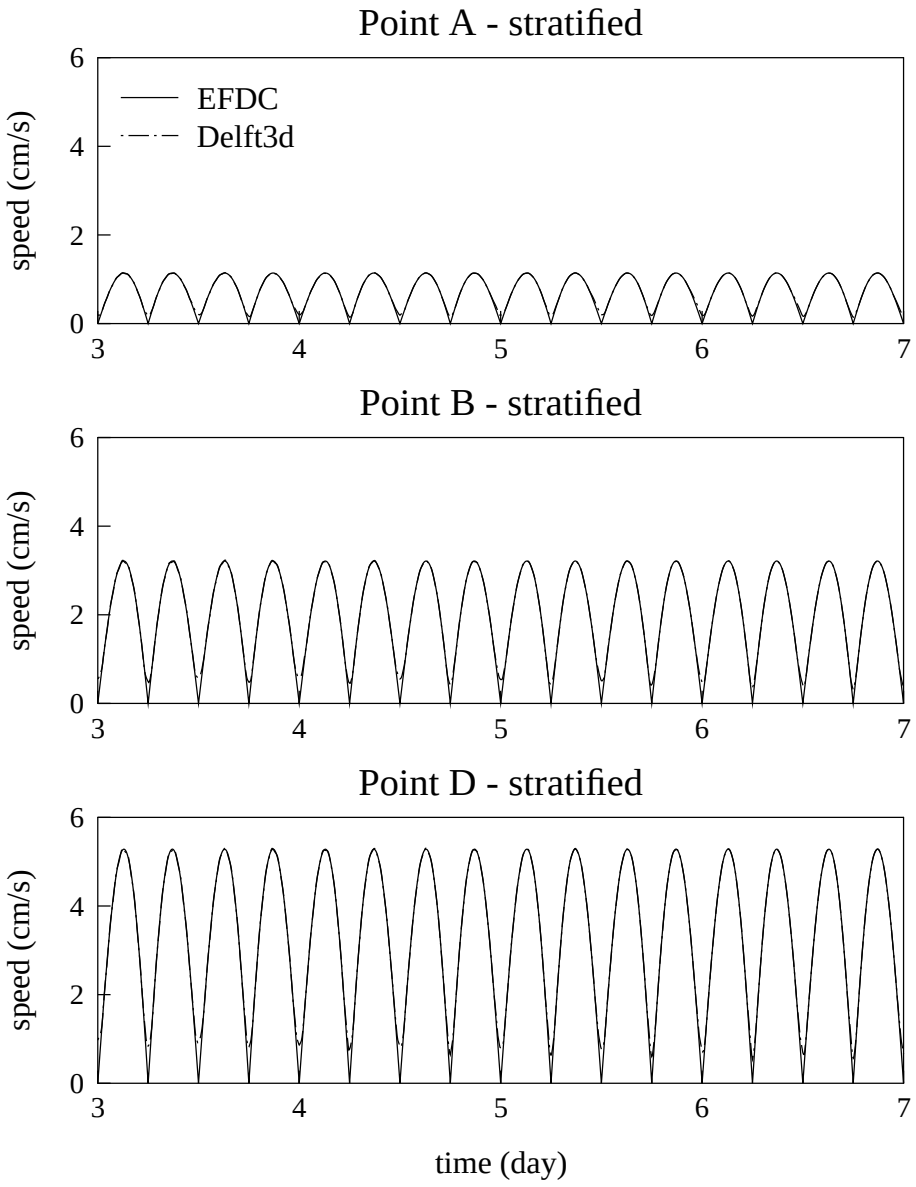

Figure 8: Computed speed for stratified tidal flow in rectangular channel

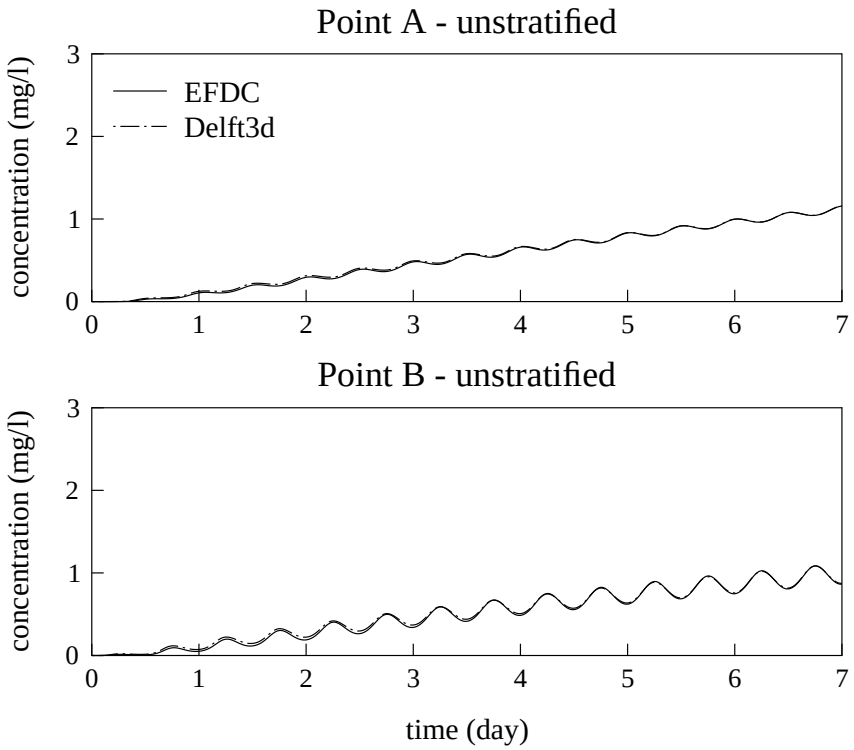

Figure 9: Computed tracer concentrations at point A and B for unstratified case with uniform source throughout the depth

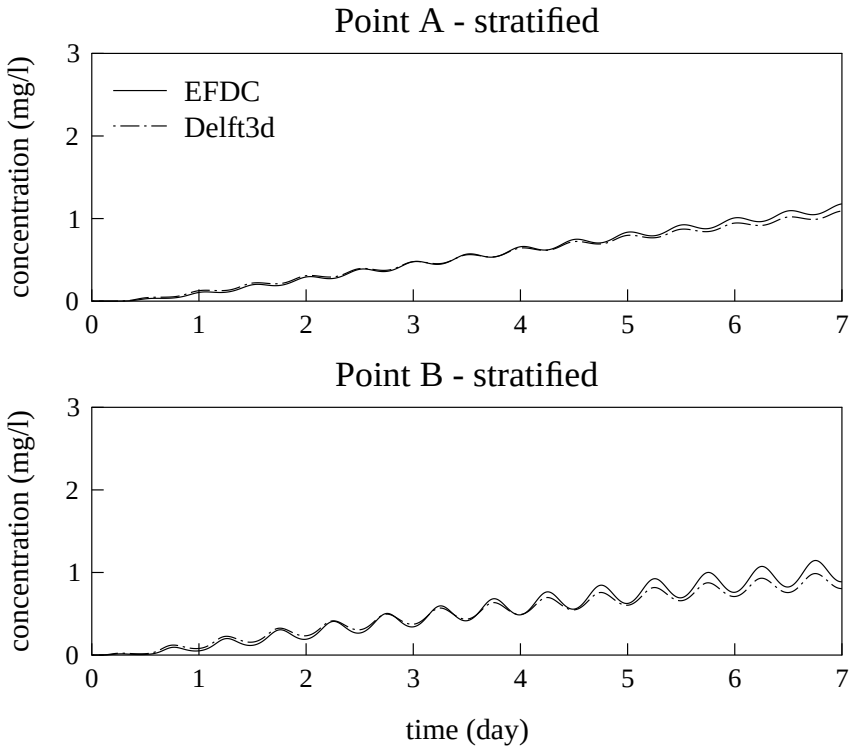

Figure 10: Computed tracer concentrations at point A and B for stratified case with uniform source throughout the depth

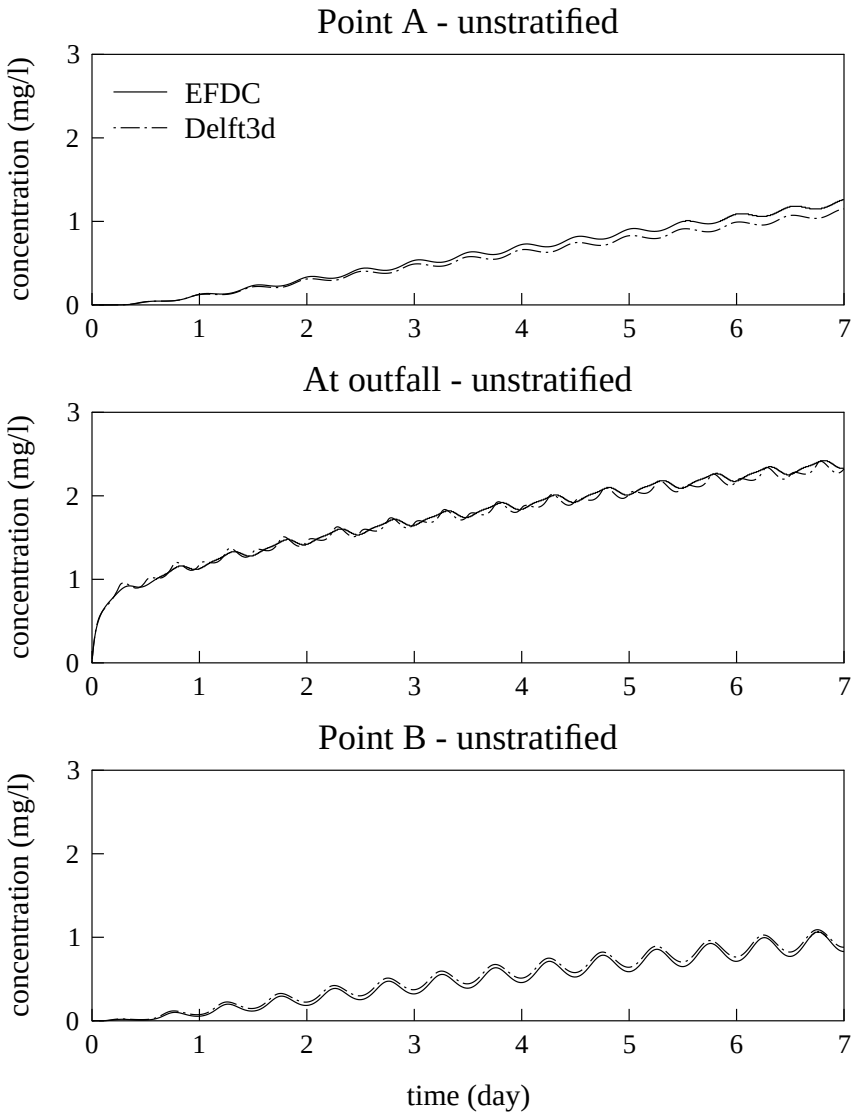

Figure 11: Computed tracer concentrations at point A and B for unstratified case with surface source

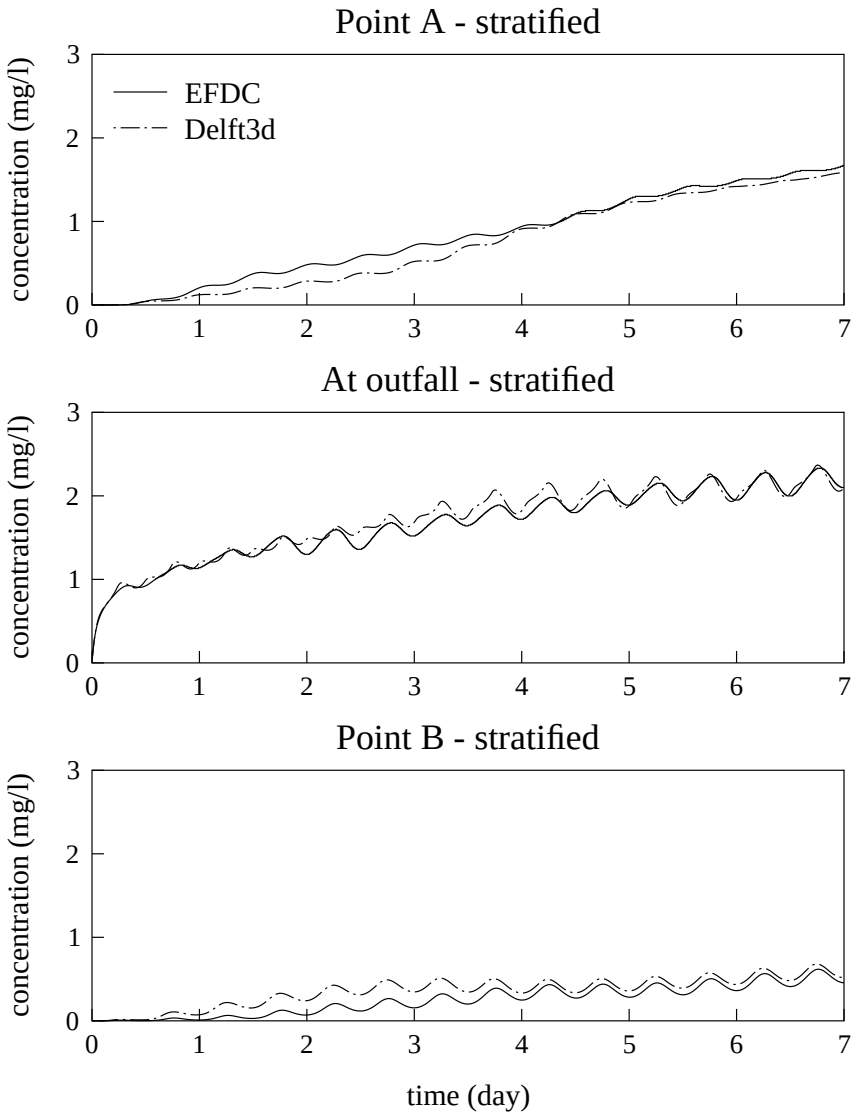

Figure 12: Computed tracer concentrations at point A and B for stratified case with surface source

4 Tolo Harbour

The basic Tolo Harbour model uses a 58 × 41 × 10 uniform grid and has 6800 active cells (Fig. 13). Each horizontal cell is 250 m × 250 m. The tidal forcing at the open boundary is assumed to be a M2 tide with amplitude of 0.85 m and period of 12.4 hours.

a) Verification with field observation - 19 August 1978

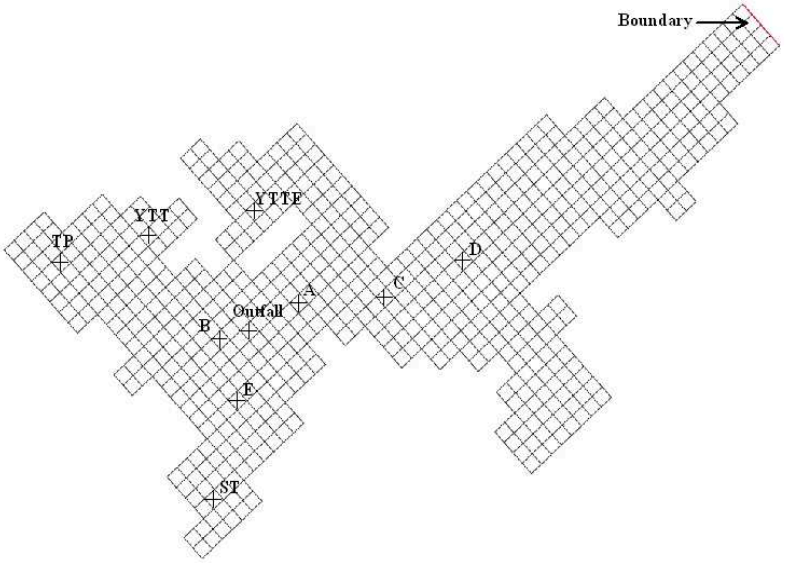

Figure 13: Model grid for Tolo Harbour

To verify the model, simulation of measured tidal condition is conducted. On 19 August 1978, a geophysical survey is conducted in Tolo Channel. Velocity profiles are measured in 3 m intervals from surface to near bottom at a station in the channel near the opening to the Mirs Bay at different tidal stages. The measurements indicate weak stratification. Continuous tidal data for the period of survey are available at the open boundary and it is approximately a semi-diurnal spring tide (Fig 14).

As there are no corresponding measurements on the vertical density profile for the same period, so the average wet season condition based on the long term salinity measurement between 1985-1996 (Fig 15) is used in the model simulation. The computed surface elevations at Taipo agreed very closely with the tidal records, and the computed velocities along the axis of the channel also compare favourably with the vertically averaged measurements in both magnitude and phase (Fig 16).

As shown in Fig 17, even though the actual density profile at the open boundary is not known, the computed vertical profiles agree reasonably well with the field measurements for different tidal stages. These support that the model developed can correctly simulate the 3D flow regime in Tolo Harbour.

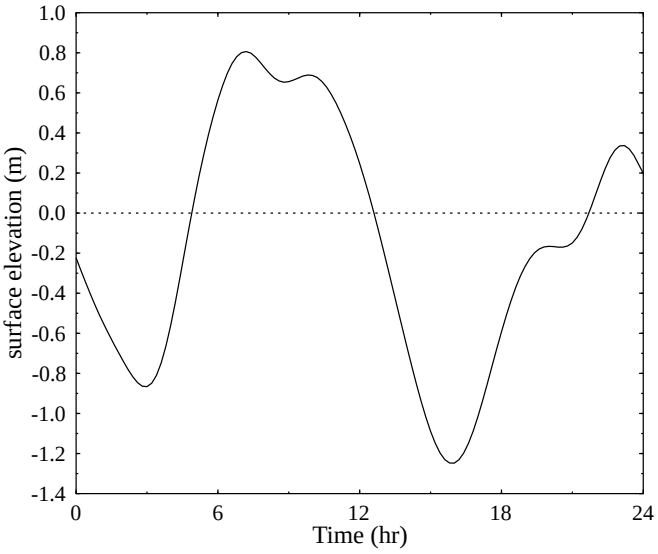

Figure 14: Input tide at open boundary of Tolo Harbour (19 August 1978)

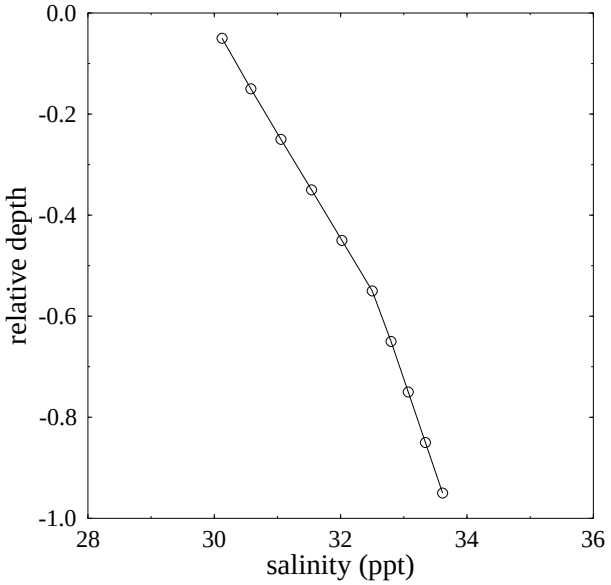

Figure 15: Vertical salinity profile (average wet season) at open boundary of Tolo Harbour

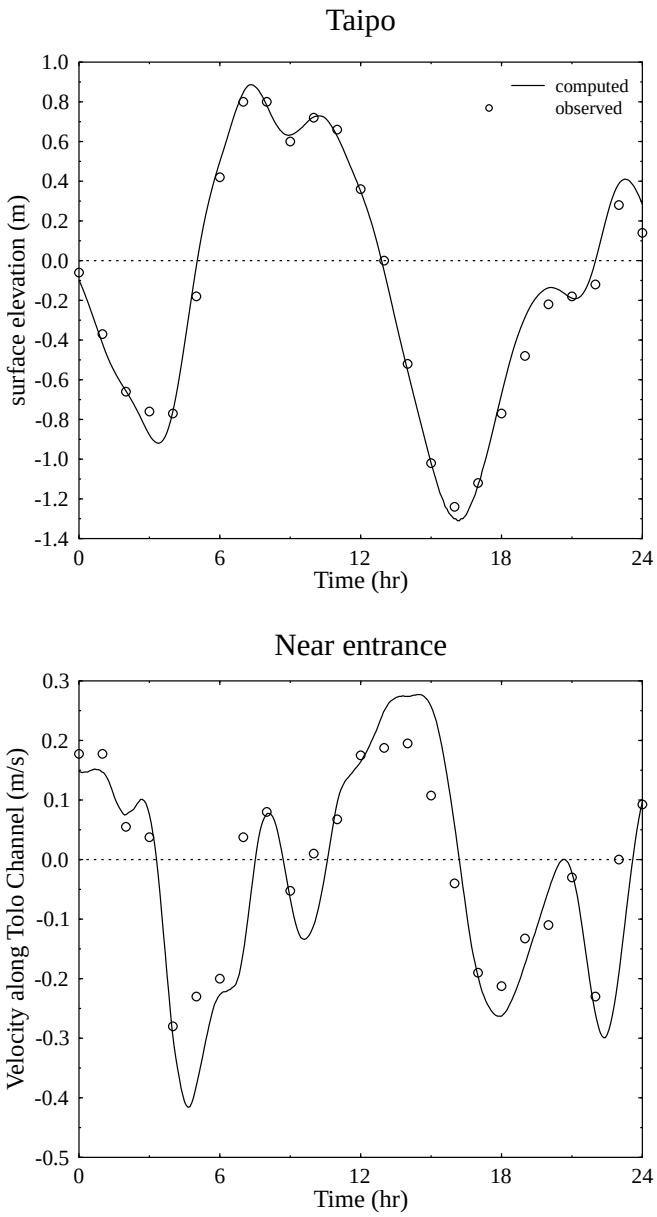

Figure 16: Comparison of predicted tides and velocities with measurements (19 August 1978)

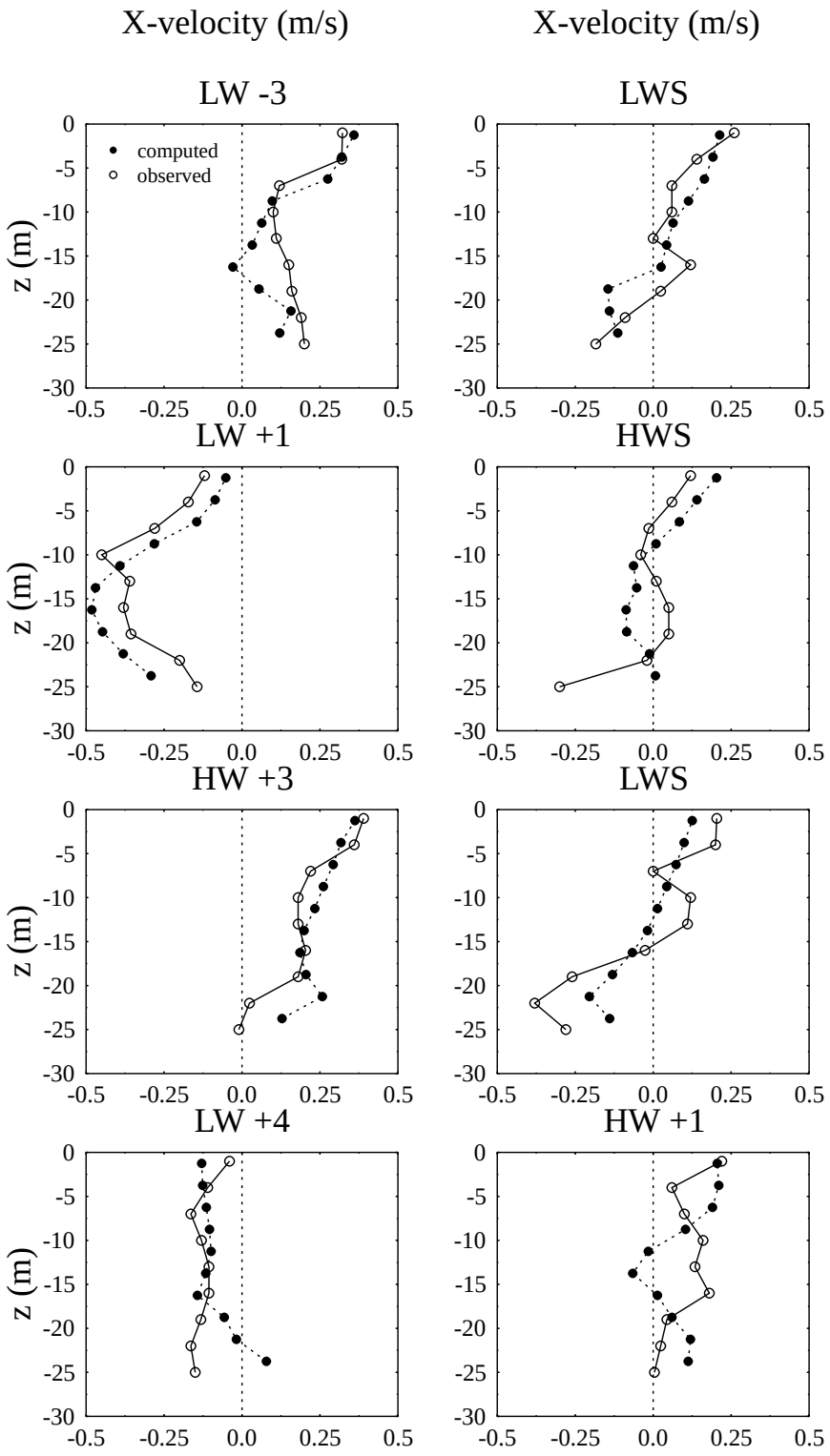

Figure 17: Computed velocity profiles at different tidal stage (19 August 1978)

b) Comparison with Delft3d - flow simulations

Two flow scenarios are carried out: unstratified and stratified case. For the unstratified case, a constant salinity of 32 ppt is considered. For stratified case, a linear vertical salinity variation is assumed at the open boundary. The surface and bottom salinity are assumed to 30 and 34 respectively (Fig. 6). The computed surface elevations and velocities by EFDC and Delft3d agree well for both the unstratified and stratified case (Fig. 18), but the EFDC results show greater tidal asymmetry than the Delft3d results (Fig. 19 - 20). The computed depth-averaged flow field during peak flood and ebb tide for the stratified case are shown in Fig. 21 - 22

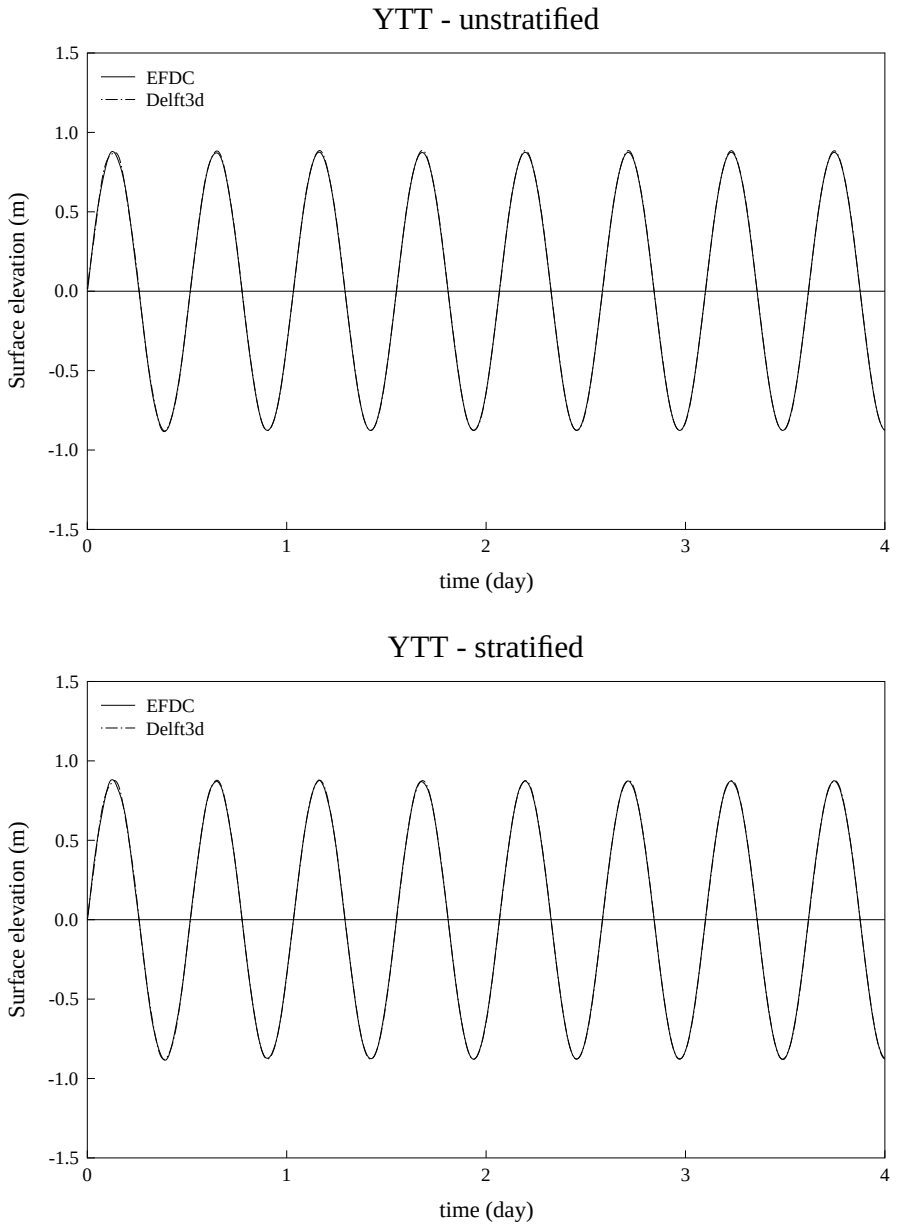

Figure 18: Computed surface elevation at Yim Tin Tsai

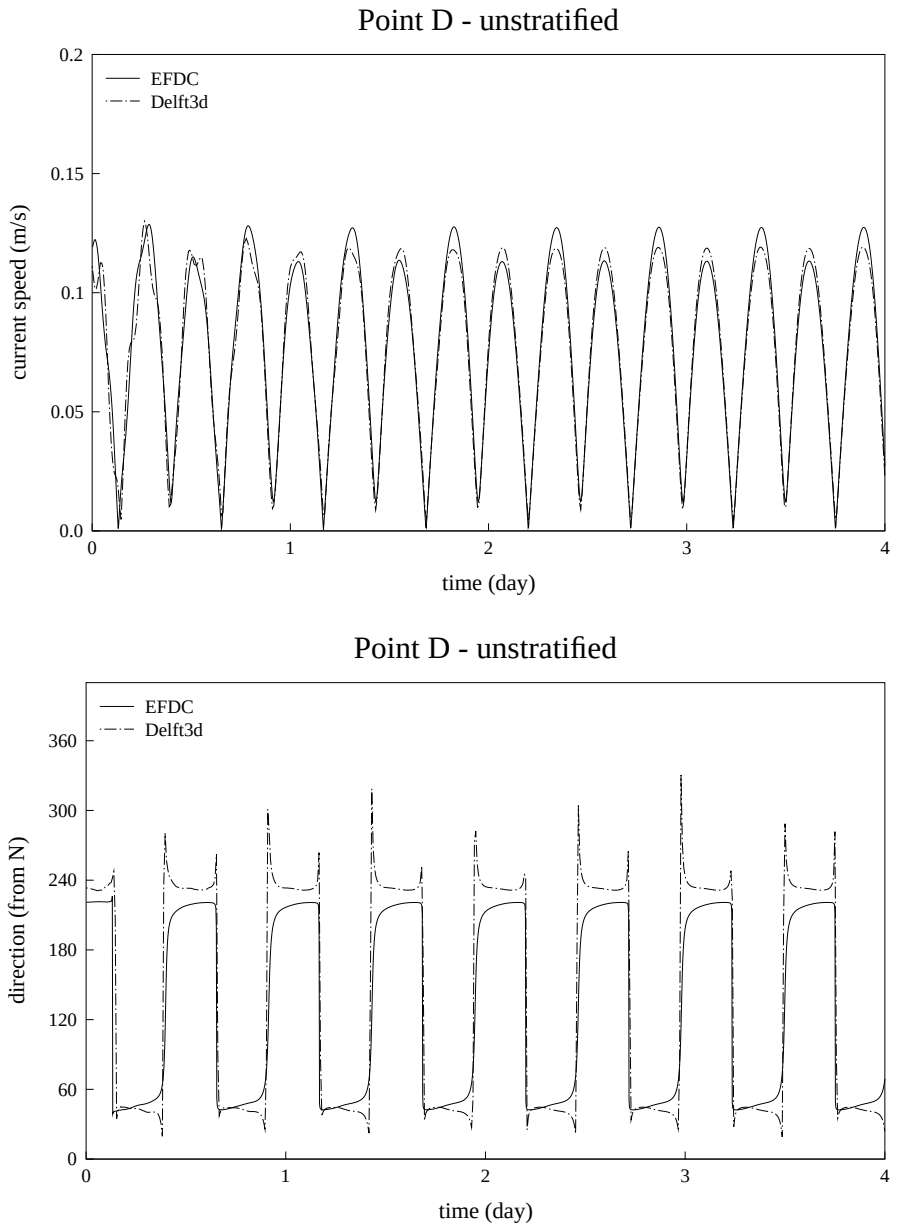

Figure 19: Computed speed and direction at point D for unstratified case

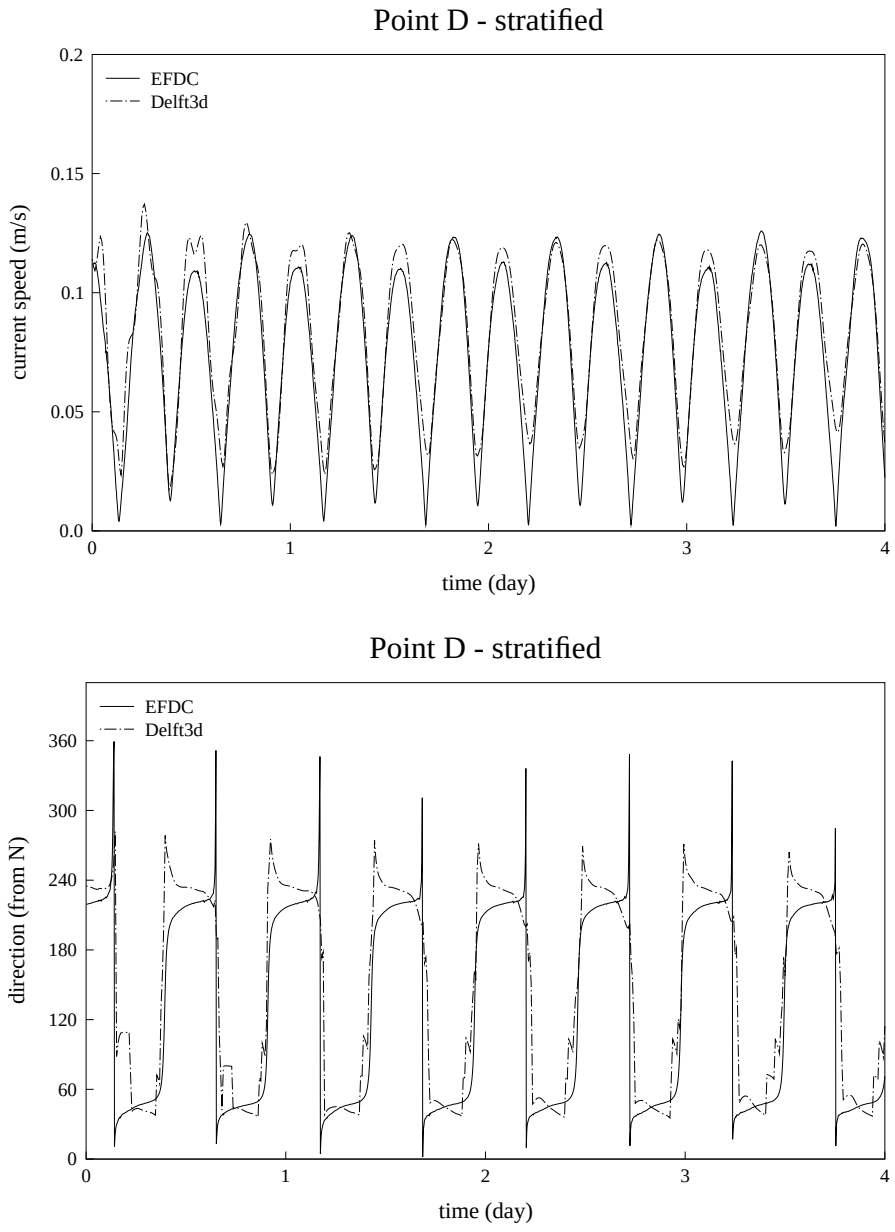

Figure 20: Computed speed and direction at point D for stratified case

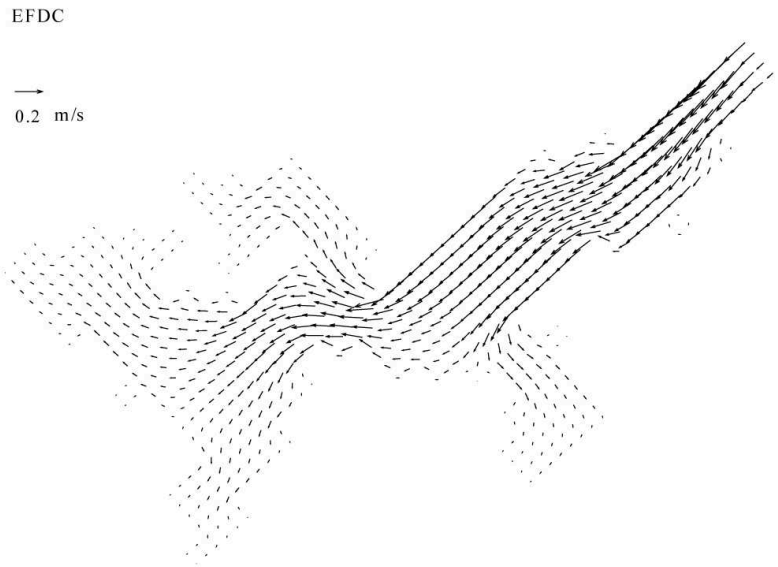

a) EFDC

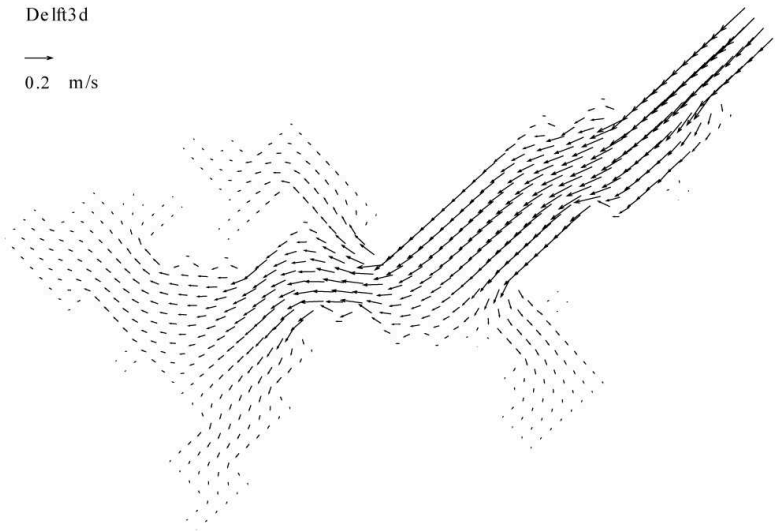

b) Delft3d

Figure 21: Computed depth-averaged velocity during peak flood for stratified case

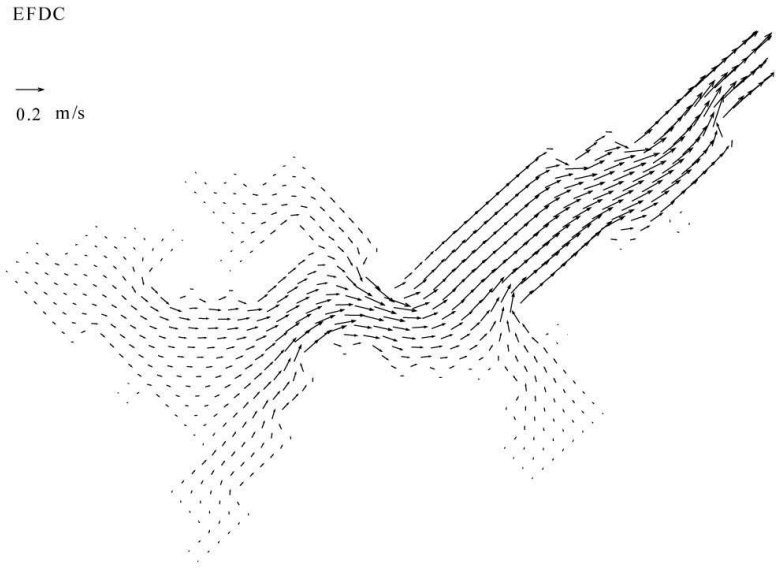

a) EFDC

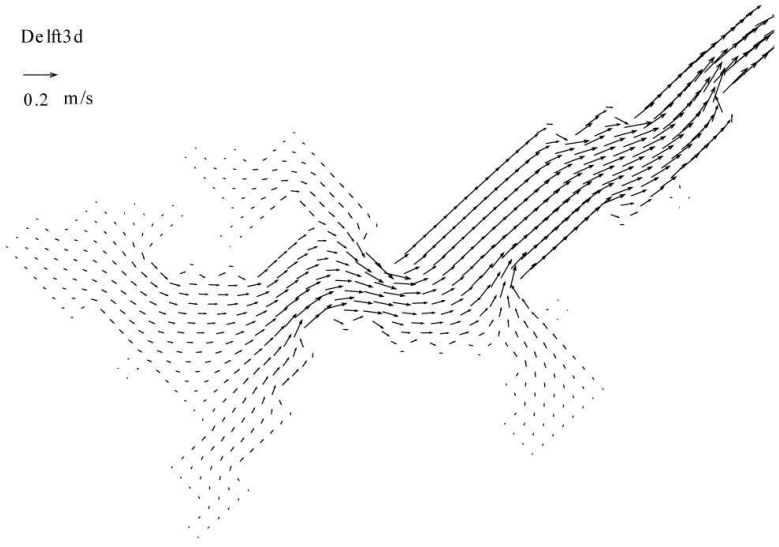

b) Delft3d

Figure 22: Computed depth-averaged velocity during peak ebb for stratified case

c) Comparison with Delft3d - water quality simulation

An outfall is assumed in the middle of the inner Tolo Harbour. An effluent discharge of 2.0 m^3/s (or 172,800 m^3/d) is employed and it is modelled as a surface discharge.

Bacteria simulation is first carried out using particle tracking approach for the unstratified case. For EFDC (with DESA), the particles are released from the last plume element in the near field simulation. For Delft3d, the particles are introduced in the surface cell. The computed results are found to agree reasonably well in both the magnitudes and variation patterns (Fig. 23- 24).

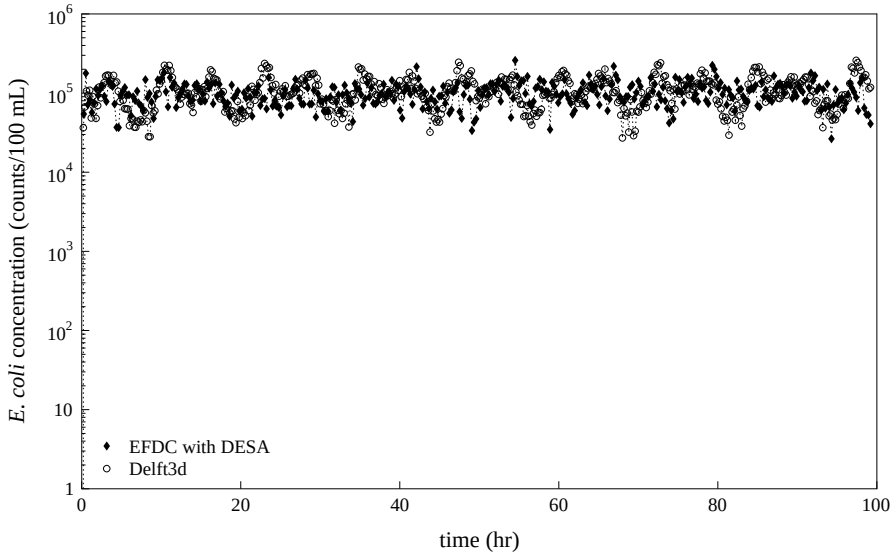

Figure 23: Computed *E. coli* concentration at the outfall

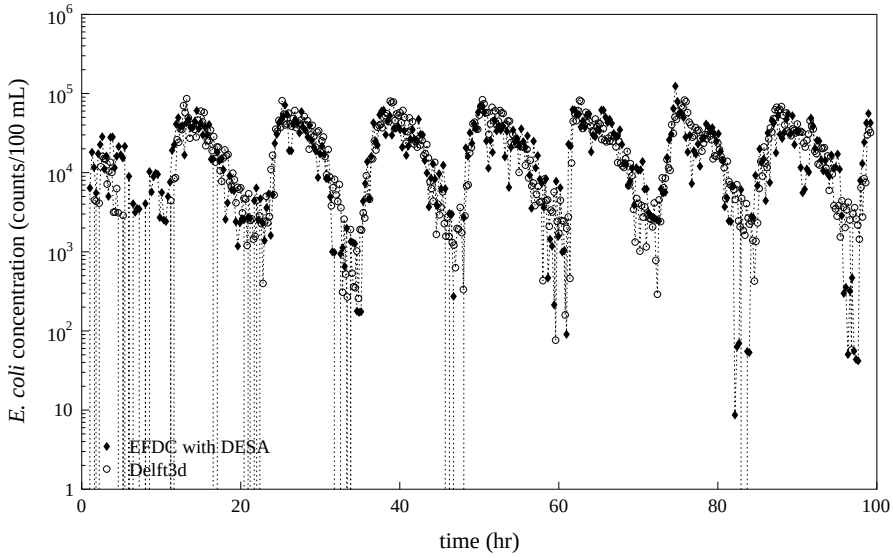

Figure 24: Computed *E. coli* concentration at point B

Water quality simulations using the mass transport are carried out for the conservative tracer and bacteria. For the conservative tracer case, the effluent concentration is taken to be 100 mg/L. For the bacteria simulation, the *E. coli* concentration is taken to be 1.1×10^7 counts/100 mL. The

decay rate parameters used are:

$k_b = 4.8\ \mathrm{d}^{-1}$, $k_s = 0.006\ (\mathrm{ppt}^{-1}\mathrm{d}^{-1})$, $\theta_T = 1.07$, $k_I = 0.0224\ (\mathrm{m}^2\mathrm{W}^{-1}\mathrm{d}^{-1})$, $I = 160\ (\mathrm{Wm}^{-2})$, $e_t = 0.08\ (\mathrm{m}^{-1})$

Hence, the corresponding mortality rate k is around 7.3 d^{-1} and equivalent to a T_{90} of about 7.6 hours.

The results of the water quality simulations agree reasonably well, especially for the unstratified case with the sources uniformly distributed through the water depth (Fig. 25 - 30). It can be seen that the computed concentrations by DESA and Delft3d agree better for the unstratified case than the stratified case, and for the case with sources distributed over the water depth than the case with the surface source.

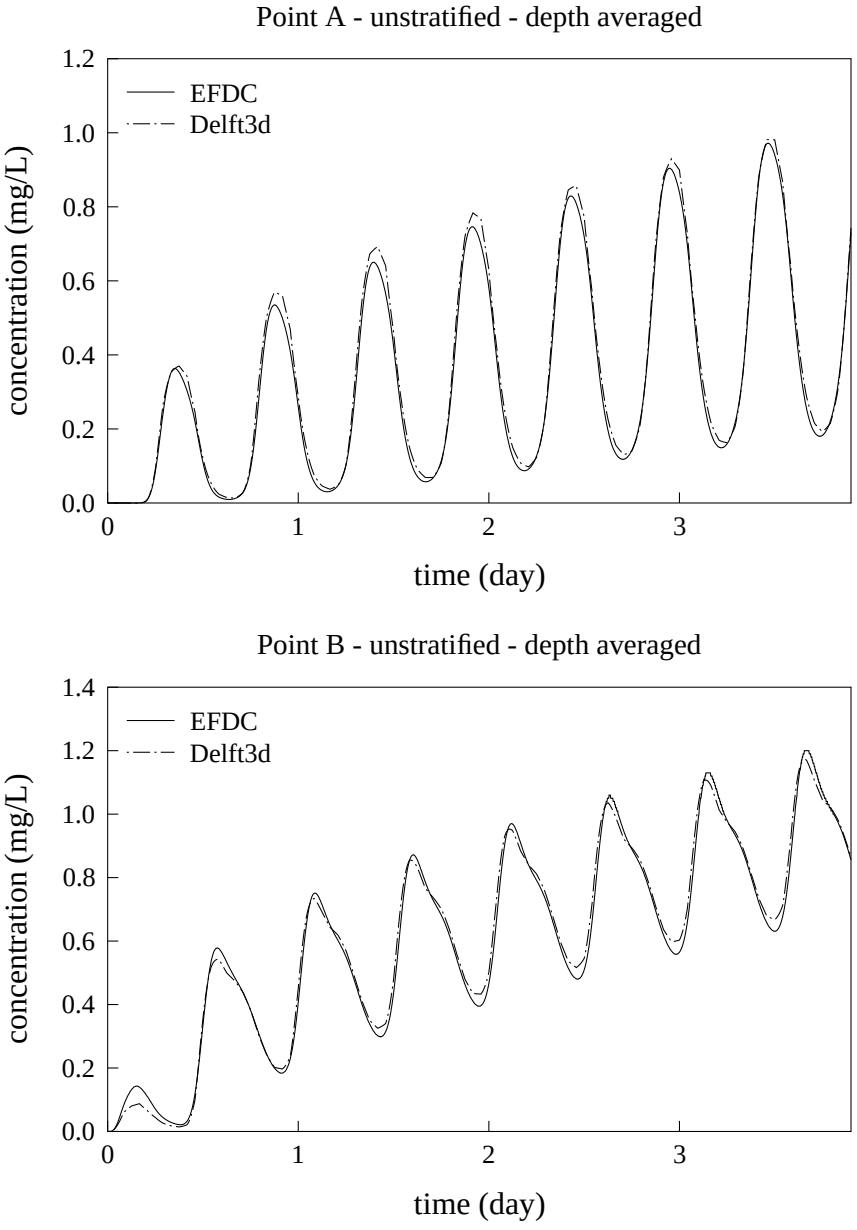

Figure 25: Computed conservative tracer concentrations at point A and B for unstratified case with uniform source throughout the depth

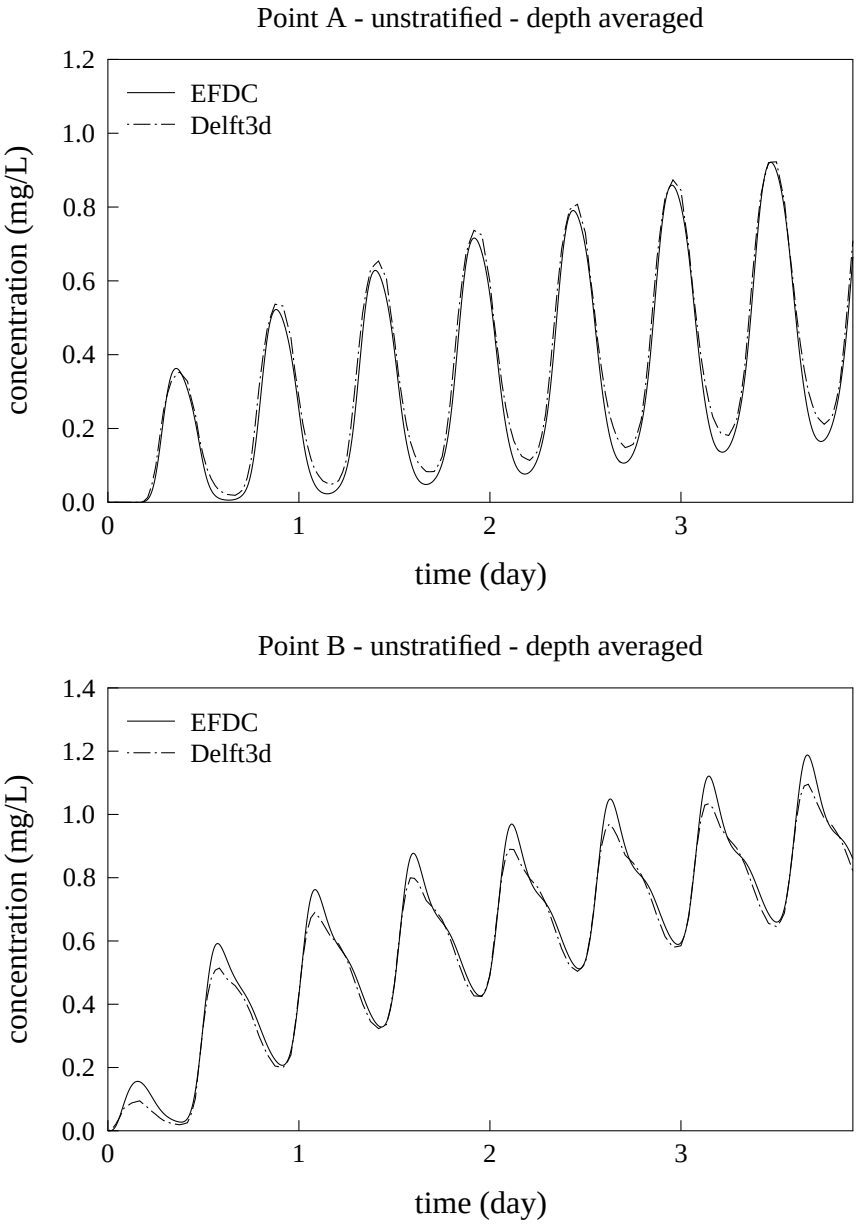

Figure 26: Computed conservative tracer concentrations at point A and B for unstratified case with surface source

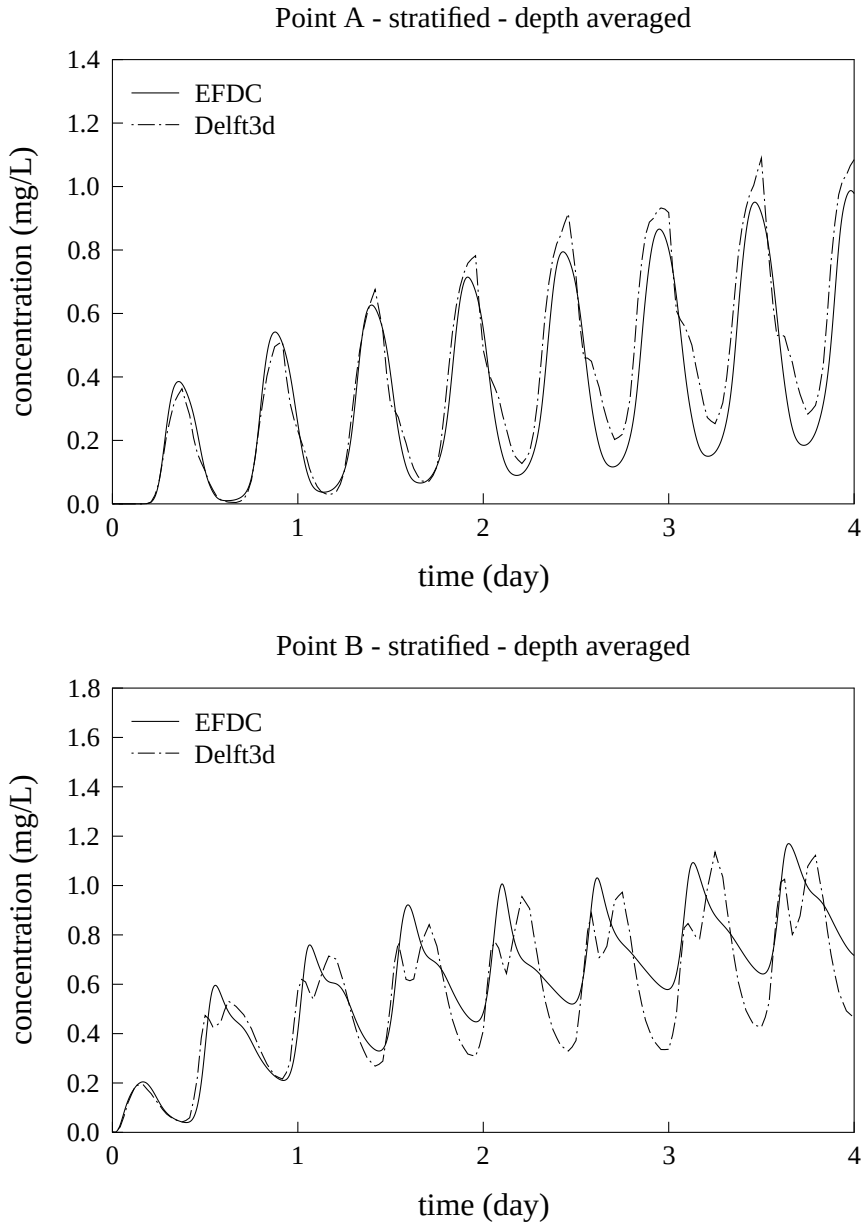

Figure 27: Computed conservative tracer concentrations at point A and B for stratified case with surface source

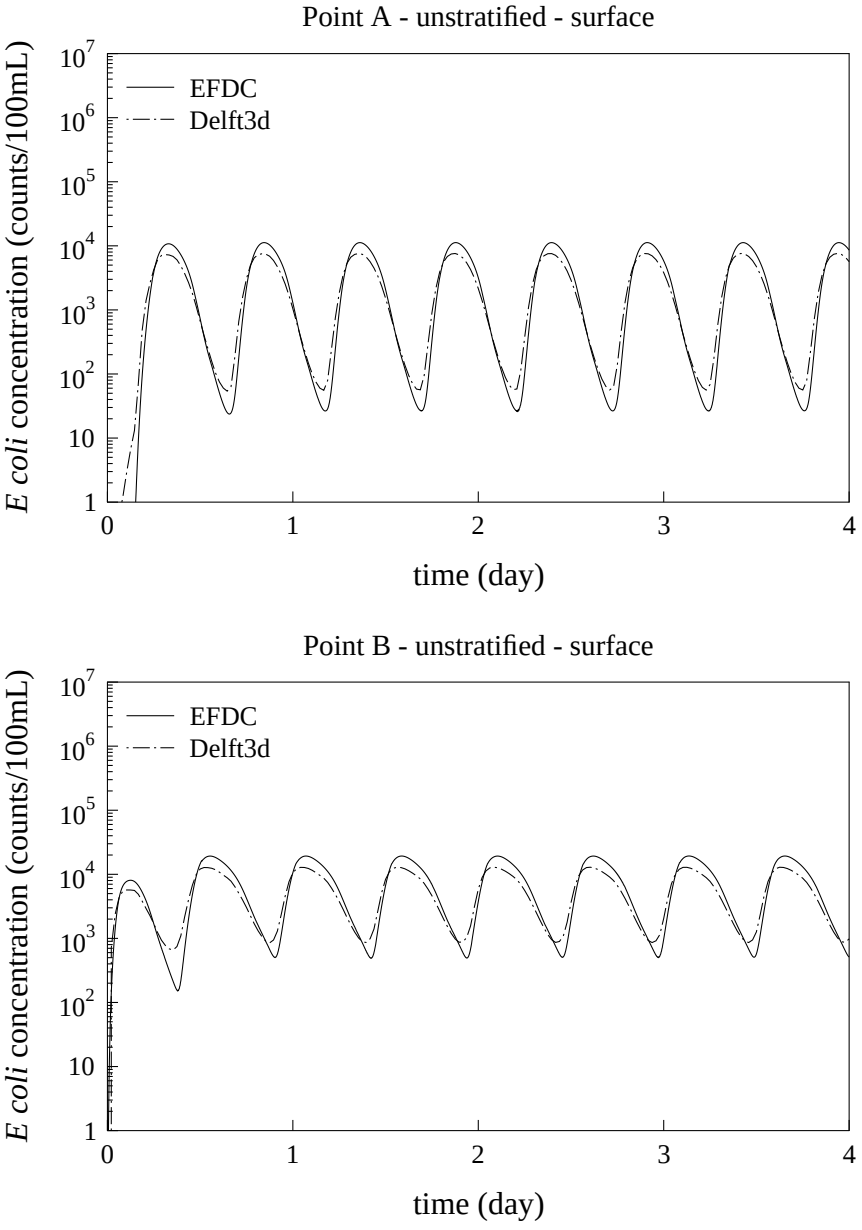

Figure 28: Computed *E coli* concentrations at point A for unstratified case with uniform source throughout the depth

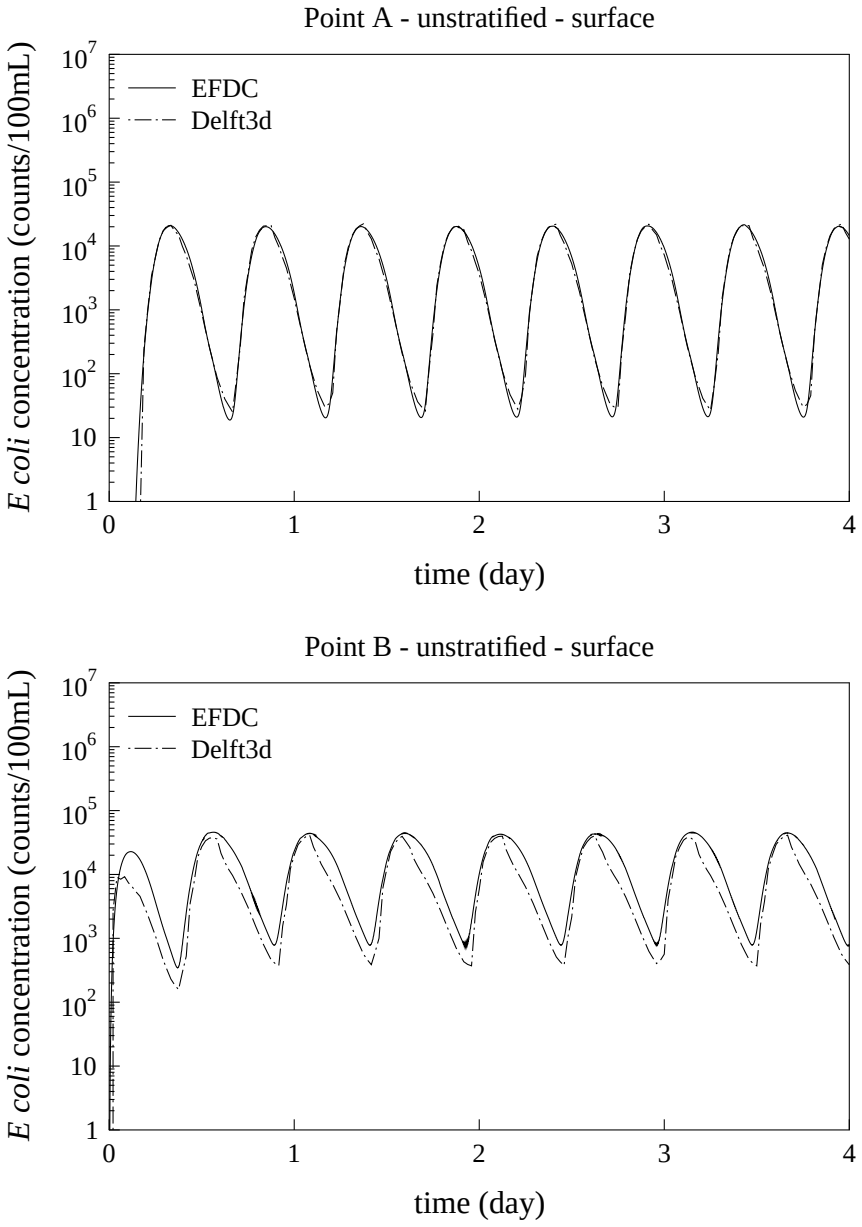

Figure 29: Computed *E coli* concentrations at point A for unstratified case with surface source

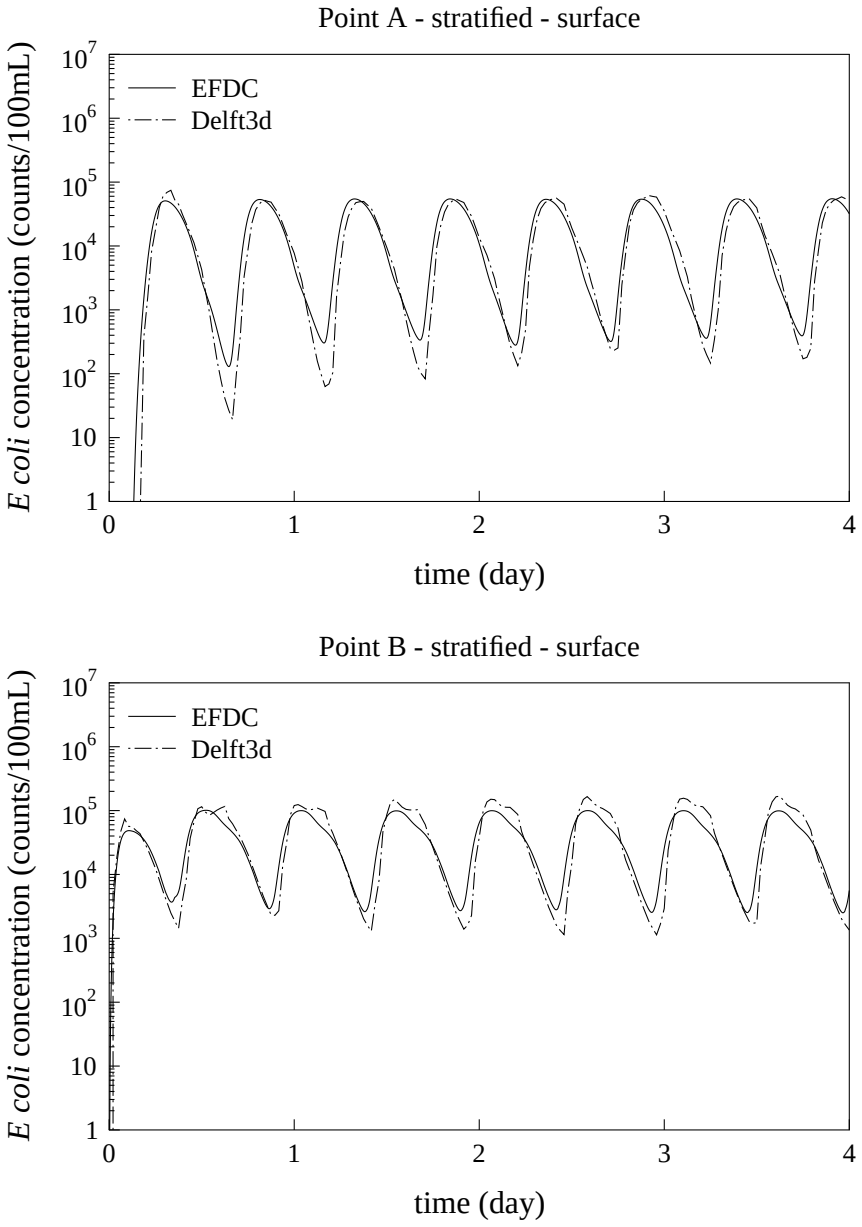

Figure 30: Computed *E coli* concentrations at point A for stratified case with surface source

5 Port Shelter

The Port Shelter model uses a 153 × 153 × 8 grid and has 100192 active cells (Fig. 31). It is a curvilinear horizontal grid and a time size of 1.0 sec. is used in the simulation runs. The Port Shelter model is driven by tidal conditions at the three open boundaries. As there is no readily available tidal constituents at those open boundary, so harmonic analysis was performed first on a time series of tidal data generated from a Delft3d model that covering the eastern part of Hong Kong waters that includes the entire Mirs Bay, Tolo Harbour and Port Shelter for the Sai Kung Sewage Treatment Works Upgrading Environmental Impact Assessment (EIA) Study. There is a total of 66 days water level data (from 27 Jul. to 30 Sep. 1996) at the boundary. These data were then used with the MATLAB program "T _ Tide" (Pawlowicz *et al.* 2002) to estimate the amplitudes and phases of the major tidal constituents. The derived tidal forcing at the open boundary is found to consist of five main tidal constituents: M2, S2, O1, P1 and K1 (Table 1). For the purpose of comparison, the amplitude and phase of these constituents derived by Hong Kong Observatory (HKO) at Quarry Bay and those adopted at the southern boundary of the Delft3d model for Hong Kong Waters. For the dry season, a vertically uniform salinity of 34 ppt is specified. For the wet season, a linearly varying salinity is assumed at the upper half of the water column (layer 1 (surface), 33 ppt; layer 2, 33.5 ppt; layer 3, 34 ppt; layer 4, 34.5 ppt) and constant at the lower half (layer 5-8, 35 ppt) are specified at the open boundaries (Fig. 32.

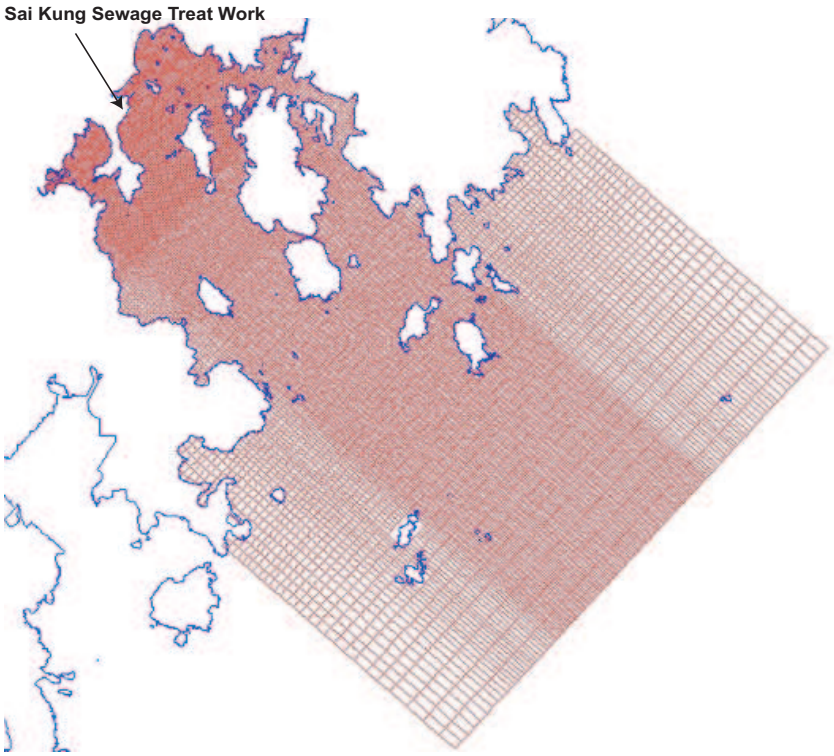

Figure 31: Model grid for Port Shelter

To validate the model against the field observation and compare with the Delft3d model, the baseline scenario representing the existing condition in 2002 is simulated. The Sai Kung Sewage Treatment Works (SKSTW) dry-weather influent flow pattern observed in mid-December 2001 was adopted to derive the 24-hour effluent flow under various design flow conditions. An average dry weather flow (ADWF) of 8,500 m^3 per day under dry season and 10,000 m^3 per day under wet season. The

Table 1: Main tidal constituents of the tidal forcing applied at the open boundary

	present study		HKO (Quarry Bay)		Delft3d HK model (south)	
Reference date					1996/07/15	
Tide	Amplitude (m)	Phase (°)	Amplitude (m)	Phase (°)	Amplitude (m)	Phase (°)
M2	0.4607	81.62	0.3964	268.0	0.3404	256.5
S2	0.1355	289.94	0.1584	296.6	0.1412	290.1
O1	0.2422	42.02	0.2964	250.8	0.2749	250.9
P1	0.1450	338.46	0.1163	294.5	0.1128	294.8
K1	0.4382	331.39	0.3663	299.7	0.3467	298.7

	Delft3d HK model (north-east)		Delft3d HK model (south-east)	
Reference date	1996/07/15		1996/07/15	
Tide	Amplitude (m)	Phase (°)	Amplitude (m)	Phase (°)
M2	0.3126	254.2	0.2926	247.2
S2	0.1380	283.7	0.1292	279.7
O1	0.2512	247.4	0.2652	248.9
P1	0.1043	295.4	0.1043	295.4
K1	0.3257	299.5	0.3257	299.5

	Delft3d HK model (north-west)		Delft3d HK model (south-west)	
Reference date	1996/07/15		1996/07/15	
Tide	Amplitude (m)	Phase (°)	Amplitude (m)	Phase (°)
M2	0.4366	272.9	0.4145	266.9
S2	0.1580	314.3	0.1485	309.3
O1	0.2880	254.0	0.3040	257.2
P1	0.1090	296.8	0.1090	296.8
K1	0.3460	301.1	0.3460	301.1

diffuser outfall for SKSTW is modelled by 6 vertical jets with a diameter of 0.26 m. The effluent discharge flow is taken to be fresh water with zero salinity. The effluent *E. coli* and conservative tracer concentration are 1500 counts/100 mL and 20 mg/L. For the bacteria simulation, the same set of parameters for the bacterial decay listed in Section 4 are used. Therefore, the bacterial mortality rate, k, used is around 7.3 d^{-1} (equivalent to a T_{90} of about 7.6 hours). Besides the effluent from SKSTW, pollution loads from other local sources (13 stormwater outfalls) are also included (Fig. 34 and Table 2).

Fig. 35 - 36 show the computed current speeds at the three EPD marine monitoring stations in dry and wet season by EFDC and Delft3d model. It can be seen that they gave good comparison throughout the spring-neap cycle. The computed conservative tracer concentrations at the three stations are shown in Fig. 37 - 38. The spatial and temporal variations agree reasonably well, but with the predicted concentrations by the Delft3d model are higher than those predicted by EFDC model.

The observed and computed averaged *E. coli* concentrations are shown in Table 3 and Fig 39. It is can be seen that the observed spatial variations for *E. coli* levels among the three marine monitoring stations (from 1998 to 2006) can be reproduced by the model. Fig. 40 shows the

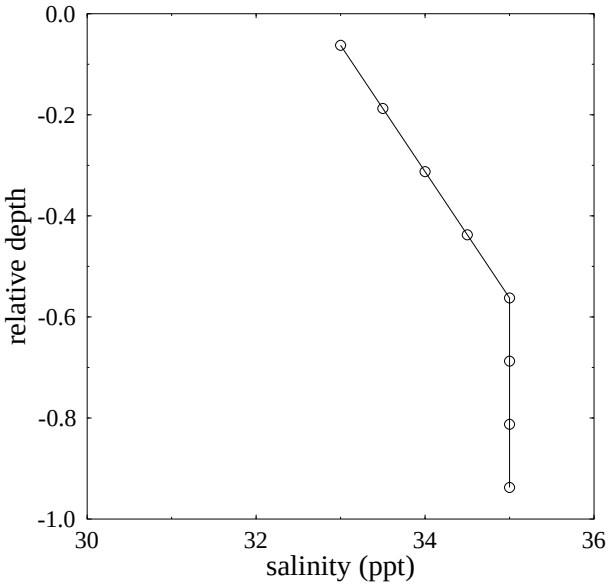

Figure 32: Vertical salinity profile for typical wet season at open boundary for Port Shelter

comparison between the computed *E. coli* at PM2 and by EFDC and Delft3d. Again, the predicted concentrations by the Delft3d model are higher than those predicted by EFDC model, but with similar varying patterns with time.

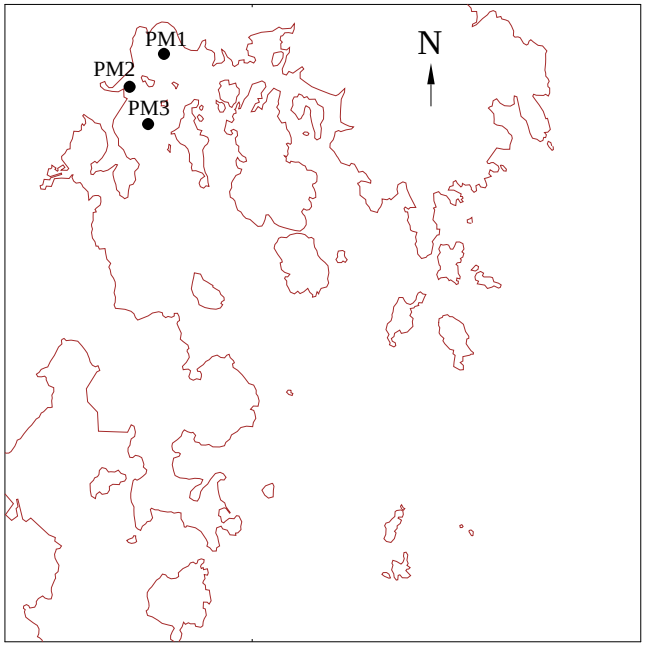

Figure 33: Location of EPD marine monitoring stations

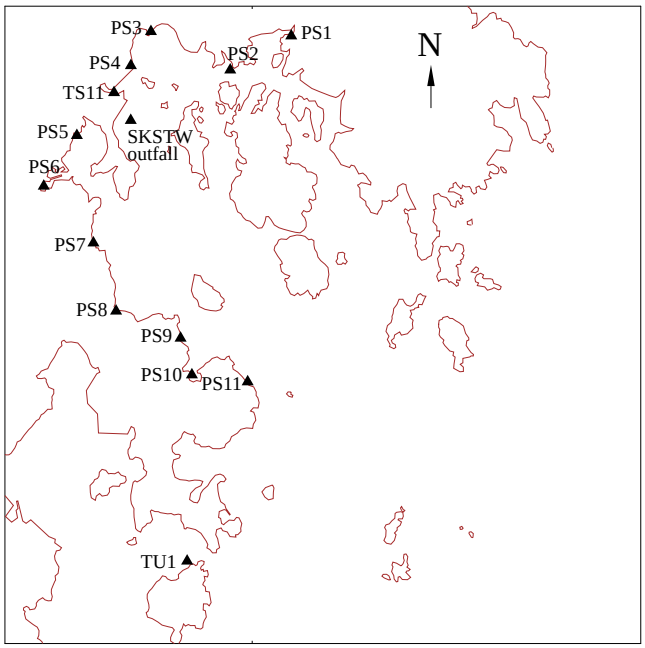

Figure 34: Location of sewage and storm outfalls

Table 2: Pollution loads applied for wet and dry season

	Dry season			Wet season)		
	Flow (m^3/s)	Tracer (mg/L)	*E. coli* (counts/100 mL)	Flow (m^3/s)	Tracer (mg/L)	*E. coli* (counts/100 mL)
SKSTW outfall	0.09838	20.0	1.0×10^7	0.11574	20.0	1.0×10^7
PS1	0.00675	51.3	1.9×10^6	0.06684	22.1	1.9×10^5
PS2	0.00675	51.3	1.9×10^6	0.06684	22.1	1.9×10^5
PS3	0.00675	51.3	1.9×10^6	0.06684	22.1	1.9×10^5
PS4	0.01895	46.5	2.4×10^6	0.19339	21.5	2.4×10^5
PS5	0.01451	46.5	1.9×10^6	0.12821	21.9	2.2×10^5
PS6	0.01451	46.5	1.9×10^6	0.12821	21.9	2.2×10^5
PS7	0.00955	51.8	2.5×10^6	0.04219	26.3	5.8×10^5
PS8	0.00955	51.8	2.5×10^6	0.04219	26.3	5.8×10^5
PS9	0.00955	51.8	2.5×10^6	0.04219	26.3	5.8×10^5
PS10	0.00955	51.8	2.5×10^6	0.04219	26.3	5.8×10^5
PS11	0.00955	51.8	2.5×10^6	0.04219	26.3	5.8×10^5
TS11	0.00094	281.4	2.8×10^7	0.00094	281.4	2.8×10^7
TU1	0.00094	509.0	4.8×10^7	0.00129	367.5	3.5×10^7

Table 3: Comparison between the observed and computed *E. coli* concentrations at EPD marine monitoring stations

Parameter	Station		dry season		wet season	
			observed ($N = 54$)	computed ($N = 360$)	observed ($N = 54$)	computed ($N = 360$)
surface *E. coli* (counts/100mL)	PM1	G.M.	1.4	< 1	1.9	< 1
		Median	1.0	< 1	1.0	< 1
	PM2	G.M.	3.3	2.8	4.7	5.1
		Median	2.5	2.1	3.0	5.1
	PM3	G.M.	1.3	< 1	1.8	< 1
		Median	1.0	< 1	1.0	< 1

dry season: October - March; wet season: April - September; G.M. - geometric mean

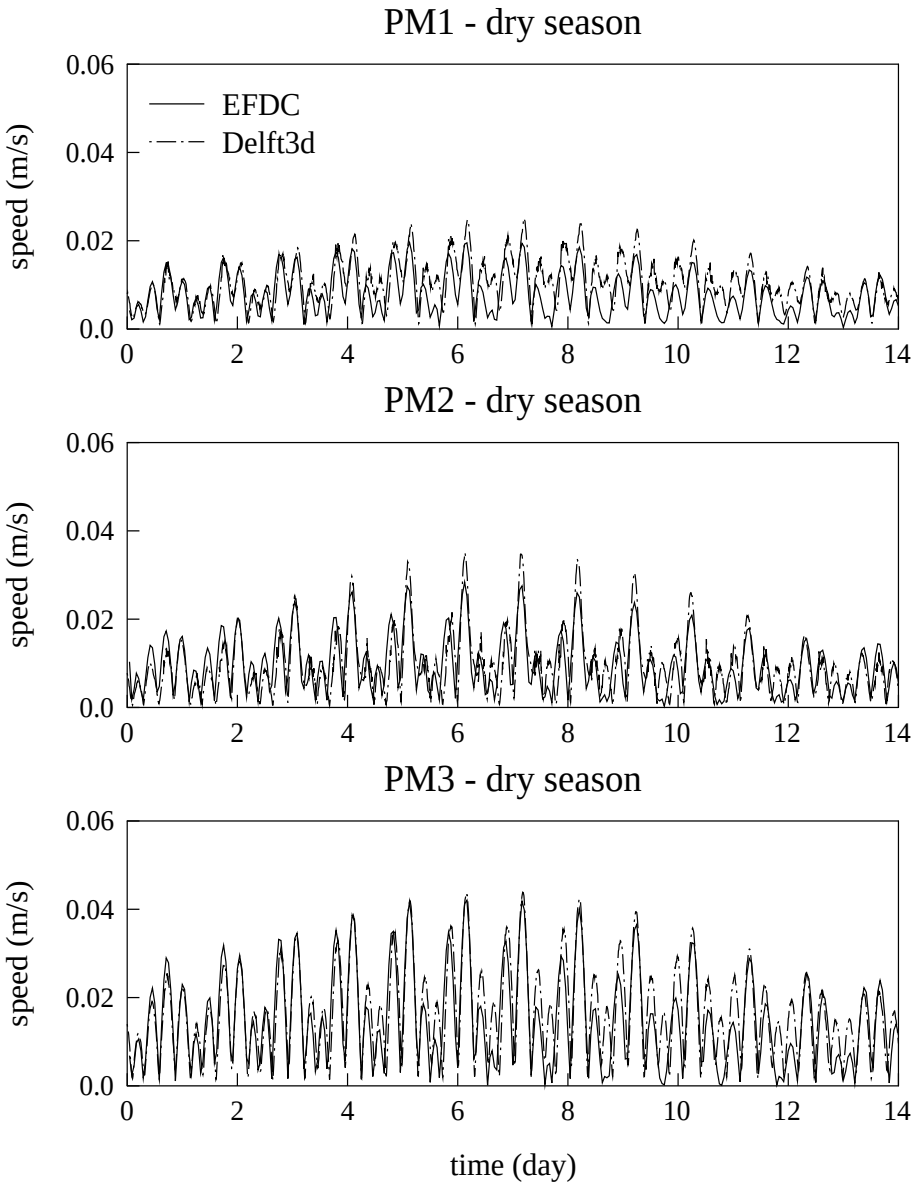

Figure 35: Computed speed at station PM1 - PM3 for dry season

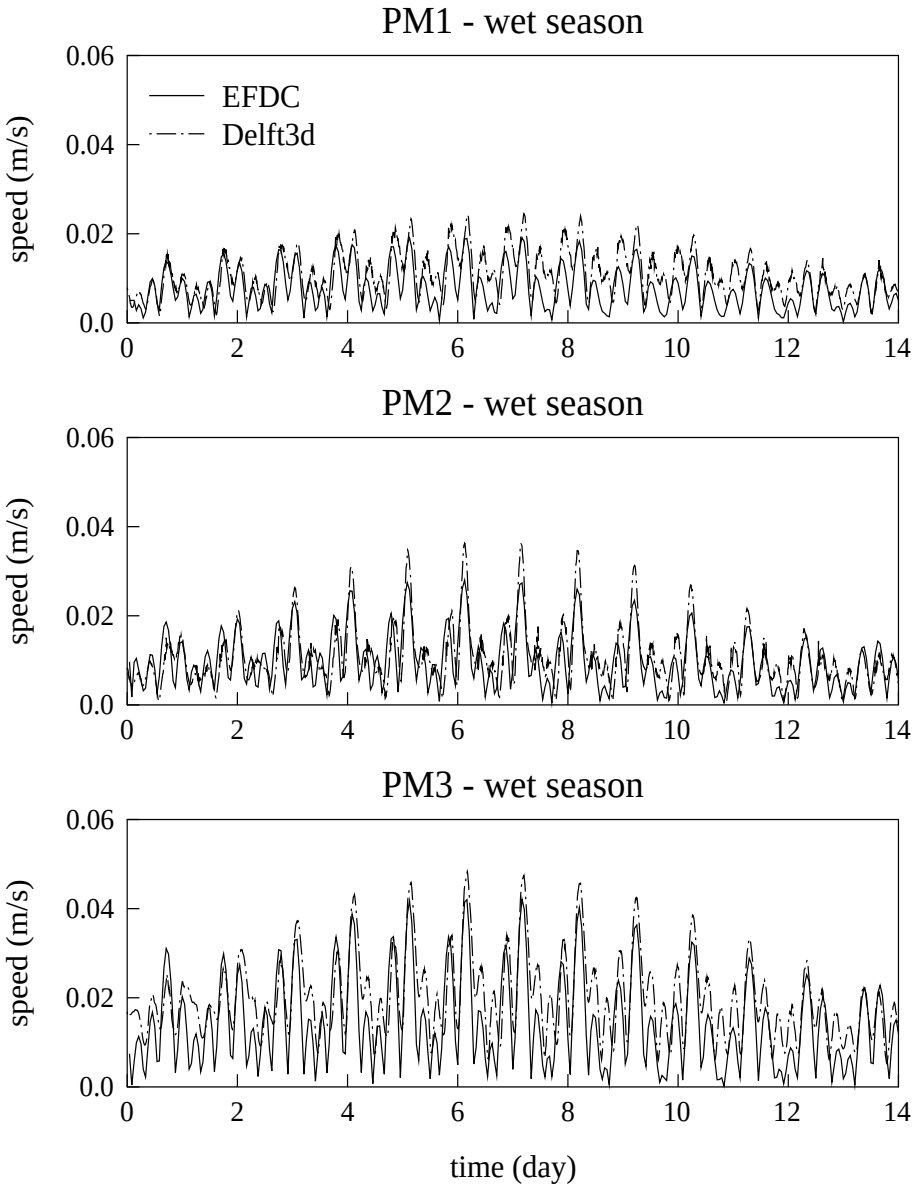

Figure 36: Computed speed at station PM1 - PM3 for wet season

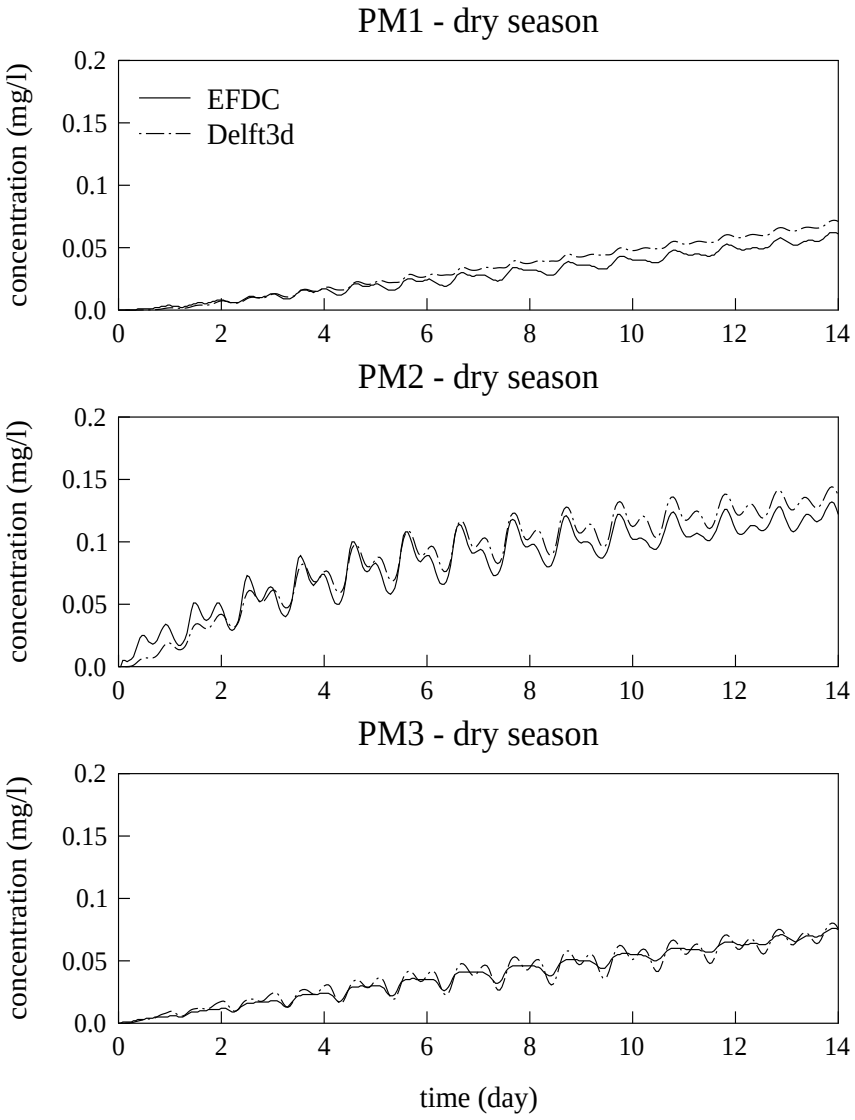

Figure 37: Computed conservative tracer concentrations at station PM1 - PM3 for dry season with surface source

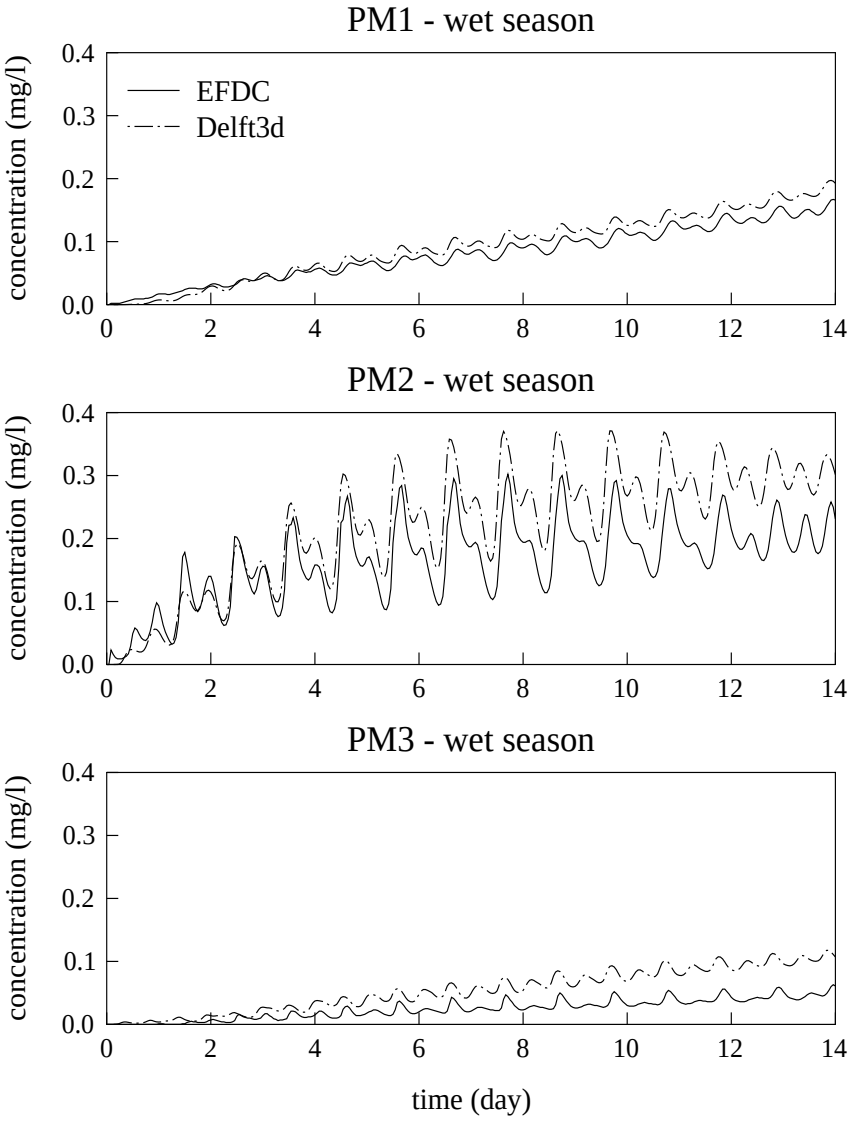

Figure 38: Computed conservative tracer concentrations at station PM1 - PM3 for wet season with surface source

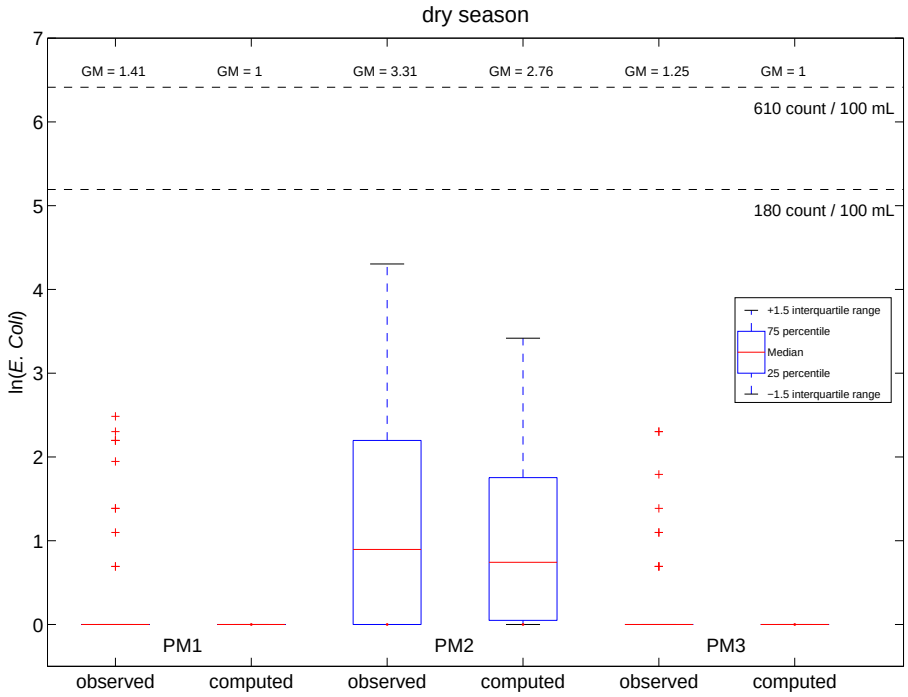

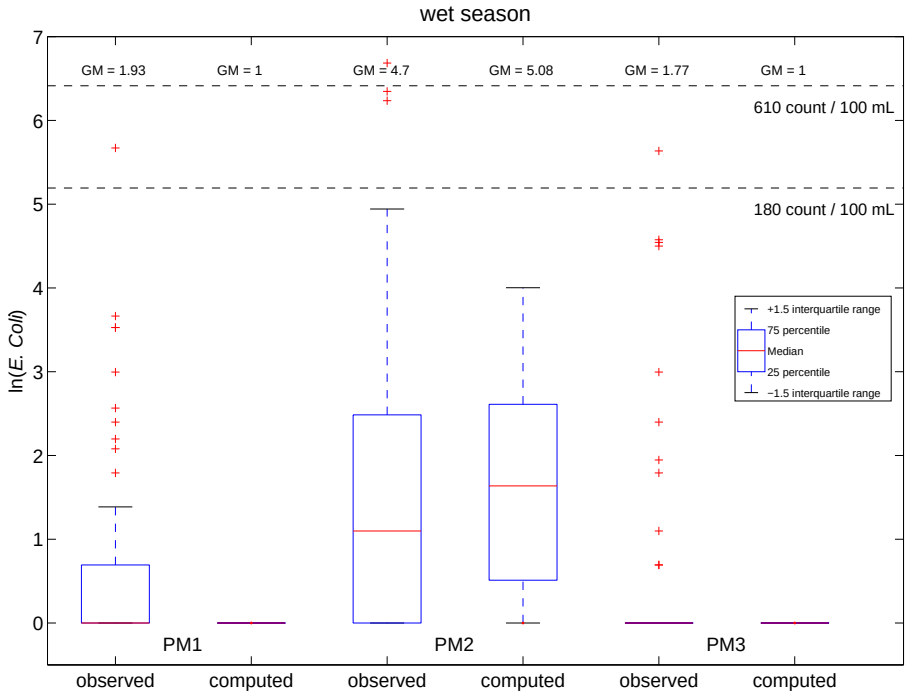

Figure 39: Comparison between the observed and computed *E. coli* concentrations at EPD marine monitoring stations

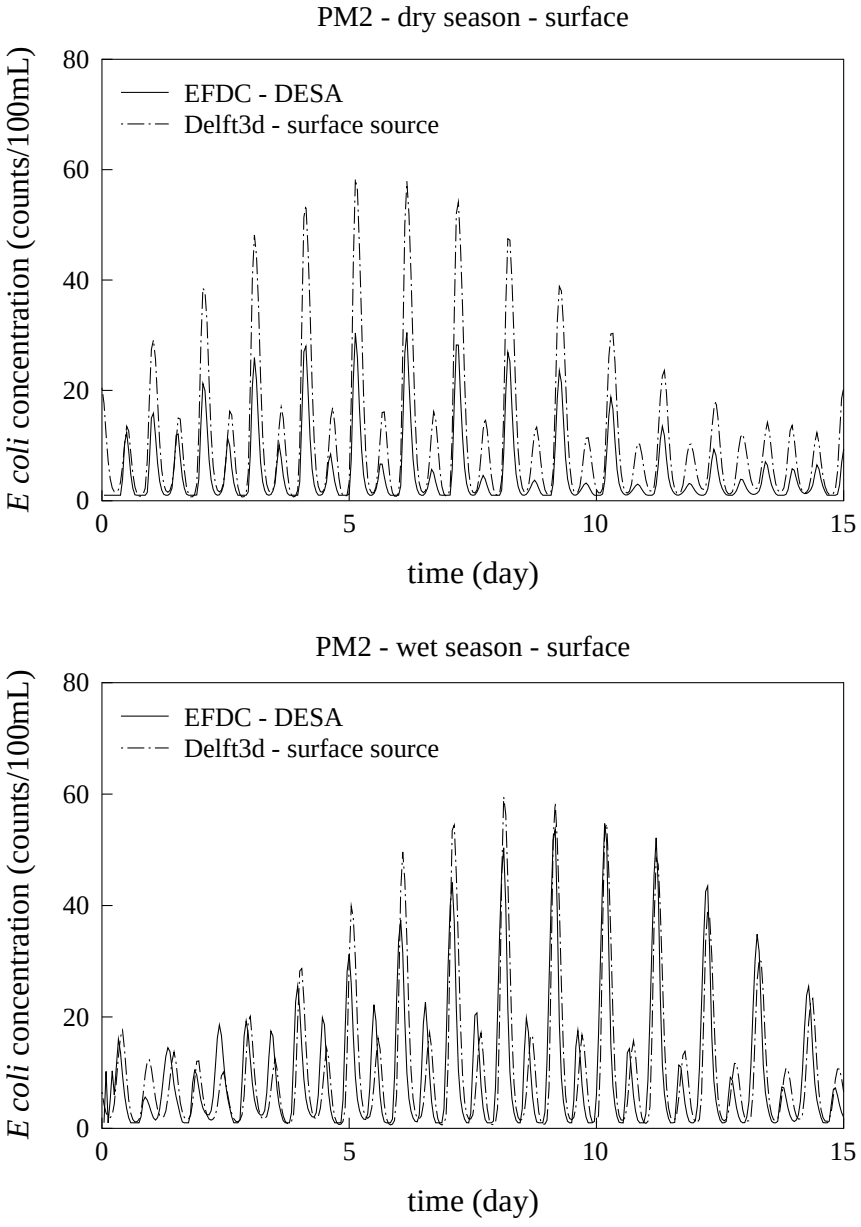

Figure 40: Computed *E. coli* concentrations at PM2

References

[1] Choi, K.W. and Lee, J.H.W., (2007). "Distributed entrainment sink approach for modelling mixing and transport in the intermediate field", *Journal of Hydraulic Engineering*, ASCE, Vol. 113, No. 7, 804-815.

[2] Delft Hydraulics, (1998). *Upgrading of the water quality and hydraulic mathematical models, Final Model Calibration and Validation Report*, Technical Services Division, Civil Engineering Office, Hong Kong SAR Government, Hong Kong.

[3] Hamrick, J.M., (1992). *A Three-dimensional Environmental Fluid Dynamics Computer Code: Theoretical and Computational Aspects*, The College of William and Mary, Virginia Institute of Marine Science, Special Report 317, Virginia, USA.

[4] Ippen, A.T. and Harleman, D.R.F., (1961), *One-dimensional Analysis of Salinity Intrusion in Estuaries*, Technical Bulletin No. 5, Committee on Tidal Hydraulics, Corps of Engineers, U.S. Army.

[5] Mancini, J.L., (1978). "Numerical estimates of coliform mortality rates under various conditions", Journal WPCF, 2477-2484.

[6] Mellor, G. L. and Yamada, T., (1982). "Development of a turbulence closure model for geophysical fluid problems", *Reviews of Geophysics and Space Physics*, Vol. 20, No. 4, pp. 851-875.

[7] Pawlowicz, R., Beardsley, B. and Lentz, S., (2002). "Classical tidal harmonic analysis including error estimates in MATLAB using T _ TIDE", *Computers and Geosciences*, Vol. 28, pp. 929V937.